Palaeogeography, Palaeoclimatology, Palaeoecology 437 (2015) 117–131

Contents lists available at ScienceDirect

Palaeogeography, Palaeoclimatology, Palaeoecology

journal homepage: www.elsevier.com/locate/palaeo

Holocene climate change in central–eastern Brazil reconstructed using pollen and geochemical records of Pau de Fruta mire (Serra do Espinhaço Meridional, Minas Gerais)

Ingrid Horák-Terra [a,1], Antonio Martínez Cortizas [b,2], Cynthia Fernandes Pinto da Luz [c,3], Pedro Rivas López [b,2], Alexandre Christófaro Silva [d,4], Pablo Vidal-Torrado [a,*]

[a] Departamento de Ciência do Solo, Escola Superior de Agricultura "Luiz de Queiroz" – ESALQ/USP, Piracicaba, SP, 13418900 Brazil
[b] Departamento de Edafología y Química Agrícola, Universidad de Santiago de Compostela - USC, Santiago de Compostela, 15782, Spain
[c] Núcleo de Pesquisa em Palinologia, Instituto de Botânica da Secretária do Meio Ambiente de São Paulo – IBt/SP, São Paulo, SP, 04301902, Brazil
[d] Departamento de Engenharia Florestal, Universidade Federal dos Vales do Jequitinhonha e Mucuri – UFVJM, Diamantina, MG, 39100000, Brazil

ARTICLE INFO

Article history:
Received 4 April 2014
Received in revised form 1 July 2015
Accepted 20 July 2015
Available online 30 July 2015

Keywords:
Peatlands
Histosols
South America Monsoon Systems
Central–eastern Brazil
Pollen
Geochemistry

ABSTRACT

Studies dealing with the reconstruction of Holocene climate change of tropical areas are scarce. Of these, multi-proxy investigations using peatlands are still absent. In this paper, we present the Holocene record of environmental changes in central–eastern Brazil reconstructed from a core sampled in Pau de Fruta mire (Serra do Espinhaço Meridional, Brazil). We combined palynological and geochemical analyses, supported by core stratigraphy, ^{14}C dating and multivariate statistics. The location of the mire is ideal because it is in an area which is directly associated with the South Atlantic Convergence Zone (SACZ). Six main phases of change suggested by vegetation and local and regional landscape dynamics were described. In phase I (~10,000–7360 cal. yr BP) the climate was very wet and cold and was accompanied by soil instability in the mire catchment (severe local erosion) and the 8.2 ka event was easily recognizable by a large increase in the deposition of regional dust. Phase II (~7360–4200 cal. yr BP) was characterized by wet and warm conditions, catchment soil stability and enhanced deposition of regional dust. In phase III (~4200–2200 cal. yr BP), climate was dry and warm and soil erosion in the catchment increased again. In phase IV (~2200–1160 cal. yr BP) dry and punctuated cooling was reconstructed, together with enhanced deposition of regional dust. Phase V (~1160–400 cal. yr BP) reflects sub-humid climatic conditions (like the current climate), the lowest inputs of local and regional dust and the largest accumulation of peat in the mire. While in phase VI (< ~400 cal. yr BP) sub-humid conditions continued but both local and regional erosion significantly increased. Our results demonstrate that the tropical peatlands of Serra do Espinhaço Meridional contain relevant records of Holocene climate changes, and that a multi-proxy approach offers good opportunities for a detailed reconstruction of palaeoenvironments.

1. Introduction

Precipitation in the Serra do Espinhaço Meridional is exclusively due to SACZ (South Atlantic Convergence Zone) activity, one of the main features of SAMS (South America Monsoon Systems) during the Austral summer. During the peak monsoon season in central–eastern Brazil (December–February), negative precipitation anomalies cause warm surface temperatures and an anomalous low-level cyclonic circulation, thus moisture flux is enhanced (Grimm, 2003; Grimm et al., 2007) and precipitation increases.

Over the Holocene, precipitation variability in this system is controlled by two main factors: *millennial-scale* and *orbital-scale*. With respect to *millennial-scale precipitation variability* the abrupt increase in monsoon rainfall is mainly related to a southward shift in the mean position of the ITCZ (Intertropical Convergence Zone; Cheng et al., 2013), whereas the structure of precipitation under *orbital-scale precipitation variability* is very complex, with changes in the SAMS intensity resulting from changes in austral summer insolation (ASI) associated with the precession cycle (Cheng et al., 2013). Due to this complexity, the reconstruction of past influences on SAMS is limited. Most of those available are based on Pleistocene records (Wang et al., 2004; Cruz

* Corresponding author at: Departamento de Ciência do Solo, Escola Superior de Agricultura "Luiz de Queiroz" – ESALQ/USP, Av. Pádua Dias, 11, 13418900, Piracicaba, SP, Brazil. Tel.: +55 19 3417 2106.
E-mail addresses: ingridhorak@yahoo.com.br (I. Horák-Terra), antonio.martinez.cortizas@usc.es (A. Martínez Cortizas), cyluz@yahoo.com.br (C.F.P. da Luz), pedro.rivas02@gmail.com (P. Rivas López), alexandre.christo@ufvjm.edu.br (A.C. Silva), pvidal@usp.br (P. Vidal-Torrado).
[1] Tel.: +55 19 3417 2106.
[2] Tel.: +34 881813379.
[3] Tel.: +55 11 5067 6101.
[4] Tel.: +55 38 3531 1811.

http://dx.doi.org/10.1016/j.palaeo.2015.07.027
0031-0182/

et al., 2005, 2009; Cheng et al., 2013; Deplazes et al., 2013), in which a larger number of climatic fluctuations can be recognized and identified.

Some authors proposed a link between changes in Holocene precipitation of the SAMS and the Bond events (Bond et al., 2001). The association of the Bond events with abrupt, centennial to millennial scale, changes in SAMS precipitation was suggested to indicate wetter conditions in the Southern Hemisphere (Arz et al., 2001; Baker et al., 2001, 2005; Ekdahl et al., 2008). For example, the oxygen isotope record of speleothems from Lapa Grande (Minas Gerais State, central–eastern Brazil), displayed abrupt fluctuations punctuating the entire Holocene (Stríkis et al., 2011), closely corresponding with Bond events 6, 5, 4 and the 8.2 cal. kyr BP. A response to Bond events 1 and 3 was not observed in those records, while other wet events at times of low IRD input to the North Atlantic occurred at 7.1 and 6.6 cal. kyr BP. Moister and cooler conditions between 9.2 and 8.0 cal. kyr BP were followed by an arid period between ca. 5.5 and 4.5 cal. kyr BP; a trend towards modern conditions (i.e. a sub-humid climate) after 4.5 cal. kyr BP has been inferred for the region of Salitre (western Minas Gerais State) from the pollen evidence (Ledru, 1993). In Lagoa Santa (central Minas Gerais State), dates for the majority of archaeological burials cluster around two peaks: 10–8 cal. kyr BP and 2–1 cal. kyr BP, with a period of 6000 years in which they are almost absent. This period is called the "Archaic Gap" and was related to a phase of abandonment of settlements and depopulation due to the onset of arid conditions (Araujo et al., 2005).

The Serra do Espinhaço Meridional (Minas Gerais State, Brazil) is located in the tropical latitudes and is one of the few mountainous regions of Brazil where peatlands have formed since the Pleistocene (Horák-Terra et al., 2014). These wetlands ecosystems are extremely sensitive to changes in hydrology and peat records have been extensively used to reconstruct changes in precipitation in the Northern Hemisphere, mostly for the Holocene (Booth et al., 2010; Chambers et al., 2010; Montero-Serrano et al., 2010), while few investigations using peat records are available for the tropics and the Southern Hemisphere in particular (Markgraf, 1985; Ledru, 1993; Markgraf and Anderson, 1994; Weiss et al., 2002; Muller et al., 2008; Daley et al., 2012).

In this study, we present a detailed reconstruction of climate and environmental change in the Serra do Espinhaço Meridional, based on a multi-proxy (stratigraphy, physical properties, pollen and geochemistry) study of a peat core sampled in Pau de Fruta mire, which comprises the whole Holocene period. The results obtained are compared with those found in the area using other environmental archives and proxies.

2. Material and methods

The PdF-I core was collected in Pau de Fruta mire (PdF) (18°15′ 270.08″S 43°40′30.64″W), Serra do Espinhaço Meridional, Minas Gerais State (Brazil) (Fig. 1). The catchment of PdF mire is elongated in a SW-NE direction and its valley is dominated by quartzitic rocks. It is the highest part of the regional mountain landscape (with maximum up to 1400 m a.s.l) and is also the headspring of a small river. The mire is narrow (10 to 80 m wide) and elongated, infilling the lower and flatter parts of the valley and overlays quartzitic sediments. The drainage of PdF is limited by quartzite structural sills oriented N–S downstream of the mire. The valley floor along the mire is only 30 m by 5 km long (0.06% slope) which, combined with limited drainage and the oligotrophic environment, generates adequate hydromorphic conditions for the development of the organic deposits studied. The talweg shows small differences in altitude and the summits are overall 15–25 m higher relative to the main drainage course. In the valley faces with higher slope (3–5%), there are shallow and sandy soils and abundant outcrops of quartzite rocks (whitish area in the Fig. 2). Colluvial–alluvial deposits are frequent. Campos (2014) found that several catchments of that region contain numerous organic deposits buried by quartzitic sandy layers in different types of mires. There is no evidence of important aeolian sedimentation in the region. Thus, the main source area for the inorganic material of the mire is the soils of the catchment; but atmospheric dust deposition may have played a more significant role in the past.

Sampling was undertaken in 2008 using a vibracore (Martin et al., 1995), and a core of 428 cm in length was recovered. The present soil is classified as a Hemic Haplosaprists (Soil Survey Staff, 2010). The basal lithology corresponds to the Sopa-Brumadinho (Grupo Guinda) formation, mostly constituted by quartzites (>90%), but also green schists and hematitic phylites (Knauer, 2007). This formation extends for more than 80 km in an E–W direction and more than 300 km in the N–S direction, and the Pau de Fruta mire is located almost at its center.

The present climate is characterized as tropical mountainous, according to Köppen classification, with an average annual precipitation of 1500 mm (Nimer, 1977). Rainfall is controlled by the activity of the South Atlantic Convergence Zone (SACZ), which is one of the most prominent characteristics of the South Atlantic Monsoon System (SAMS) during the austral summer, associated to intense convective activity in the Amazonian region (Garreaud et al., 2009). The SACZ extends in a southeastern direction from the interior of the continent to the South Atlantic (Vera et al., 2006). From the end of the monsoon period, rainfall almost ceases from May to October.

Vegetation is that typical of the Cerrado biome (savanna), one of the most endangered in the world, but also contains a mosaic of patches of tree species (seasonal semi-deciduous forest and Cerradão), called "Capões", which appear as small islands dispersed among grassland formations (wet grassland: *Campo Limpo Úmido*, dry grassland: *Campo Limpo Seco*, and rupicola-saxicolous grassland: *Campo Rupestre*).

The core stratigraphy is composed of 10 horizons and 3 basal inorganic layers (Fig. 1), which are named according to the terminology of the Soil Survey Staff (2010). They basically differ in the content of mineral/organic matter, texture of the inorganic component, degree of peat decomposition and consistency (described according to Schoeneberger et al., 1998 and FAO, 2006). The basal layers (3C, 2C e C; >404 cm) are quartzitic mineral sediments. Horizon Oa7 (404–298 cm) contains many fine roots but organic matter is highly sapric, and there are sections with higher proportions of mineral matter at 404–400 cm, 381–365 cm, 328–327 cm, 316–315 cm and 305–300 cm; charcoal (355–330 cm) and wood fragments (340 cm) were also found. Horizon Oa6 (298–278 cm) is sticky and sapric, with low fiber content, and occasional charcoal. Horizon Oa5 (278–202 cm) is also sapric, less sticky and has higher fiber content than the underlying layer; charcoal particles were found at 278–258 cm, 235–230 cm and 210–200 cm, and wood fragments at 275 cm and 255 cm. Horizon Oa4 (202–158 cm) has a large mineral content, but the material is sticky because of the sapric nature of the organic matter; scattered charcoal particles were also found. Horizon Oa3 (158–137 cm) has a lower mineral matter content than Oa4, it is less sticky and has higher fiber content, with charcoal fragments at 146–137 cm. Horizon Oa2 (137–125 cm) is also sapric, highly sticky, has low fiber content, and scattered charcoal fragments. Horizon Oe-i (125–119 cm) is hemic-fibric, with a mixture of fine and coarser fibers. Horizon Oa (119–113 cm) is sapric; no charcoal was found. Horizon Oi-e (113–60 cm) is fibric-hemic and the upper layer, Oi (60–0 cm), is highly fibric.

2.1. Palynological study

For the pollen analysis, 21 samples of 1 cm in thickness were obtained from the PdF-I core, taken every 20 cm between 0–60 cm and 63–383 cm, each 40 cm between 103 and 143 cm and each 18 cm between 383 and 401 cm. The physico-chemical treatment followed the procedure described in Ybert et al. (1992), with the addition of hydrofluoric acid for the dissolution of silicates, hydrochloric acid to eliminate fluorosilicates, acetic acid to dehydration and adding of acetolysis mixture for dissolution of the organic matter and acetylation of pollen, spores and other non-pollen palynomorphs (NPP) exine. Ultrasound

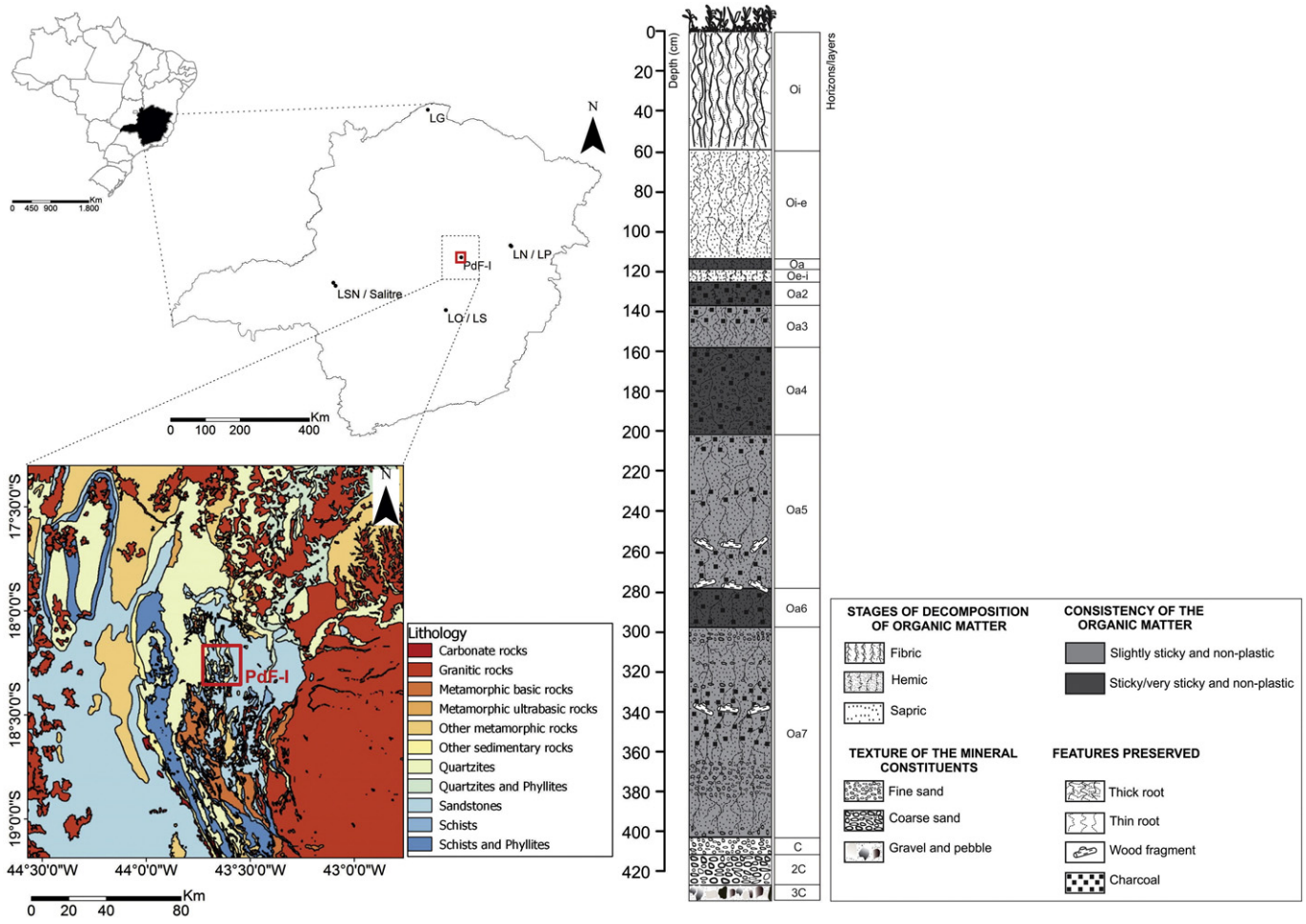

Fig. 1. Location of the Pau de Fruta mire, State of Minas Gerais, Brazil. Lithological map of the sampling location and nearby regions and stratigraphy of the PdF-I core. Other palaeoclimate records: LG (Lapa Grande; Stríkis et al., 2011); LSN (Lagoa de Serra Negra; De Oliveira, 1992); Salitre (Ledru, 1993); LN (Lagoa Nova; Behling, 2003); LP (Lago do Pires; Behling, 1995); LO (Lagoa dos Olhos, De Oliveira, 1992); LS (Lagoa Santa; Parizzi et al., 1998).

was used to separate large organic remains. Counting was undertaken at 400× under the microscope, obtaining an average total land pollen sum (TLP) of 414 terrestrial pollen grains per sample. Hydro-hygrophytes and NPP were not included in the TLP, but are expressed as percentages of it. The average sum of hydro-hygrophytes and NPP was 166 palynomorphs. Identification was aided by a reference collection

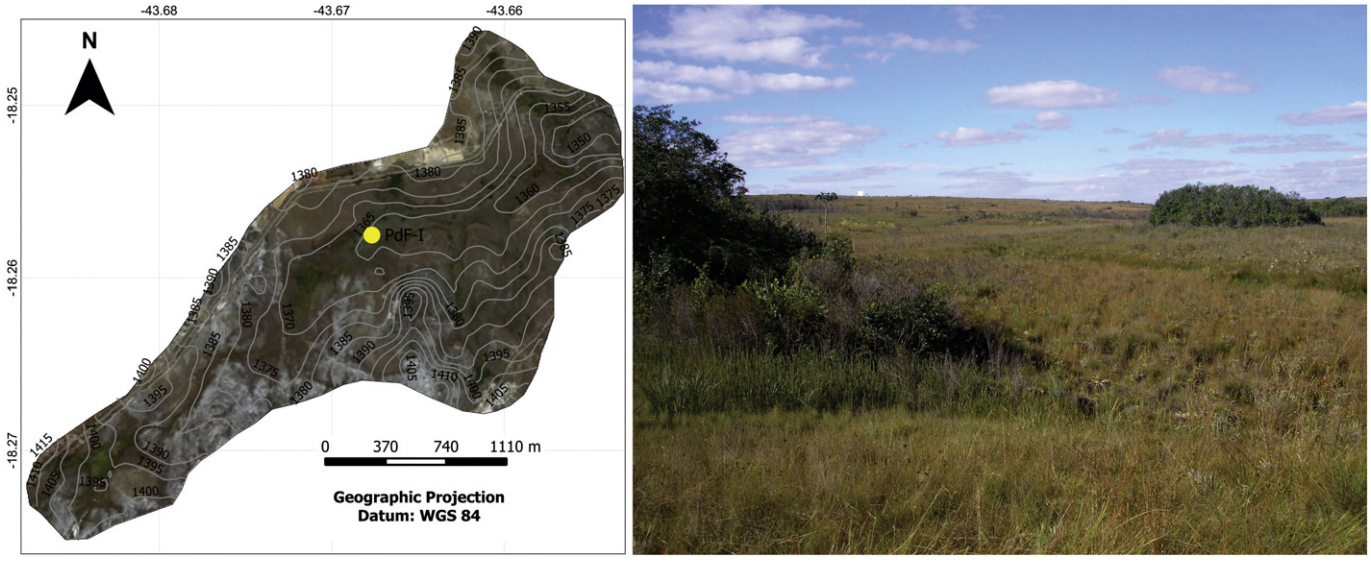

Fig. 2. Hypsographic map of the Pau de Fruta mire (yellow point is the sampling location of PdF-I core) and image of sampling location with "Capões" dispersed among grassland formations.

of the Pau de Fruta mire hosted at the laboratory of Núcleo de Pesquisa em Palinologia do Instituto de Botânica do Estado de São Paulo, Brazil, identification keys and atlases (van Geel, 1978; Tryon and Tryon, 1982; Roubik and Moreno, 1991). Taxa included in the TLP are considered to be indicators of the regional vegetation, while hydro-hygrophytes and NPP are considered to mainly provide a local signal. The NPP can be safely considered as local indicators as their dispersal is limited, however the case of the hydro-hygrophyte taxa is more complex, as they could also be part of the regional communities (López-Merino et al., 2012), as for example the Cyperaceae. Pau de Fruta is a valley mire (in an upper catchment position) and variations in the depth of the water table could be responsible for differences in the spatial distribution of local plant communities. For this reason, we have included the hydro-hygrophytes into the local signal. To support our assumptions, modern pollen rain (modern deposition) was also determined (see in Horák, 2009). Environmental requirements for regional taxa follow those described by Mendonça et al. (1998) and Marchant et al. (2002), and hydro-hygrophytes and NPP by van Geel (1978) and van Geel et al. (1989). Information about the length of the dry seasons and mean winter temperatures (MWTs) defined for the main types of vegetation from south to north Brazil was obtained from Ledru et al. (1998), to support climate inferences. Pollen diagrams were undertaken using TILIA software (Grimm, 1992).

2.2. Elemental and carbon and nitrogen isotopic composition

Carbon and N contents and isotopic composition ($\delta^{13}C$ and $\delta^{15}N$) were determined in dried, milled and homogenized peat samples of 10 cm thickness, using an elemental analyzer coupled to a mass spectrometer hosted at the Laboratório de Isótopos Estáveis of the Centro de Energia Nuclear na Agricultura - CENA/USP (Piracicaba, SP, Brasil). Major, minor and trace elements (Si, Al, Fe, Ti, S, P, Ca, K, Rb, Sr, Y, Zr, Nb, Mn, Ni, Cr, Cl, Br) were determined by X-ray fluorescence using two energy dispersive XRF analyzers (Cheburkin and Shotyk, 1996; Weiss et al., 1998) hosted at the RIAIDT facility (Infrastructure Network for the Support of Research and Technological Development) of the University of Santiago de Compostela (Spain). The instruments were calibrated using several reference materials (NIST 1515, 1541, 1547 and 1575, BCR 60 and 62 and V-1). Since the core contained both organic and inorganic layers, calibrations were performed for inorganic and organic matrices. Detection limits for organic matrices are: <0.01% for Al, Si, S, K, Ca and Fe; 0.005% for P; 0.001% for Mn; 0.0005% for Ti; 10 μg g^{-1} for Cl; 1 μg g^{-1} for Cr, Ni, Br, Rb, Sr, Y, Zr and Nb. Detection limits for mineral matrices are: 0.1% for Al; 0.05% for Si; 0.04% for K; 0.01% for Ca and Fe; 0.006% for P; 0.004% for S; 0.002% for Ti and Mn; 10 μg g^{-1} for Cl; and 1 μg g^{-1} for Cr, Ni, Br, Rb, Sr, Y, Zr and Nb. One in every five samples was analyzed in triplicate and the measurements agree within a 5% for most elements; values that did not agree within 10% were rejected (in which case more replicates were done).

2.3. Radiocarbon age dating and age/depth model

Eleven samples were radiocarbon dated by AMS in the AMS Laboratory of Georgia University (UGAMS, USA) and Beta Analytic Inc. (Miami, USA) (Table 1). The age-depth model was obtained using the Clam.R application developed by Blaauw (2010), which also performs the calibration (using the SHCal13.14C, Reimer et al., 2013). We excluded one date (that at obtained at 288 cm) as it was much younger than expected. The best fit was obtained with a smooth-spline solution (Fig. 3). In the text ages are thus provided as calibrated values unless specified otherwise. For the sake of consistency, ages found in the literature as conventional values were also converted to calibrated ones when the uncertainty term was available or assuming a ±50 uncertainty when it was not.

Table 1
Results of ^{14}C dating, showing calibrated ages (2σ) in cal yr BP.

Lab. code	Depth (cm)	^{14}C age (BP)	Age (cal yr BP)
Beta – 327639	25	108.3 ± 0.3 pM	117 ± 22 pM
UGAMS – 4921	57.5	430 ± 25	493 ± 31
UGAMS – 4922	87.5	500 ± 25	525 ± 19
Beta – 327640	92.5	300 ± 30	404 ± 57
Beta – 327641	147.5	610 ± 30	600 ± 54
Beta – 330478	204.5	4070 ± 30	4576 ± 69
UGAMS – 4920	209.5	4030 ± 30	4497 ± 75
Beta – 327642	288	4050 ± 30	5007 ± 581
Beta – 327643	348	7610 ± 40	8406 ± 56
UGAMS – 4923	396	8090 ± 30	9039 ± 54
Beta – 330479	418	9360 ± 40	10,596 ± 102

2.4. Statistical analysis

Stratigraphically constrained cluster analysis (total sum of squares method; Grimm, 1987) was applied to pollen and NPP data to define regional and local palynological zones. Principal components analysis (PCA) was also performed on the transposed data matrices of the regional and local types and NPP. This type of analysis enables an intuitive interpretation of pollen data from an ecological point of view summarizing the pollen composition of the samples based on co-variation (López-Merino et al., 2012). The pollen and NPP data were log-transformed and standardized (z-scores) before analysis, as suggested for compositional data (i.e. close data sets) (Reimann et al., 2008). The PCA was performed in the correlation mode and a varimax rotation was applied to maximize the loadings of the variables in the components (Eriksson et al., 1999). PCA was also applied to geochemical data in the same conditions as pollen data, but without transposing the data matrices. It was undertaken using SPSS 20.0 software.

3. Results

3.1. Palynological study

The synthetic pollen diagrams for the regional and local taxa and NPP are provided in Figs. 4 and 7, while the complete diagram can be found in Supplementary Figs. A.1 and A.2. Assemblages of regional pollen types are interpreted to represent phytophysionomies (based on environmental requirements, Supplementary Tables A.1 and A.2): semi-deciduous forest (*Floresta Semidecidua*), mountain forest (*Floresta Montana*), wet grasslands (*Campo Limpo Úmido*), dry grassland (*Campo Limpo Seco*), rupicola-saxicolous grassland (*Campo Rupestre*), and savanna

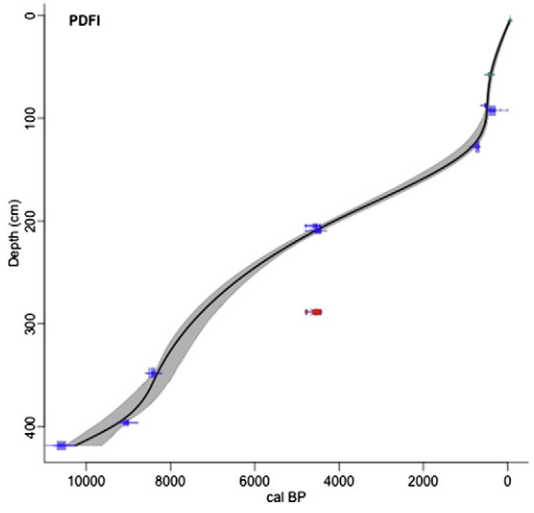

Fig. 3. Age-depth model of the PdF-I core.

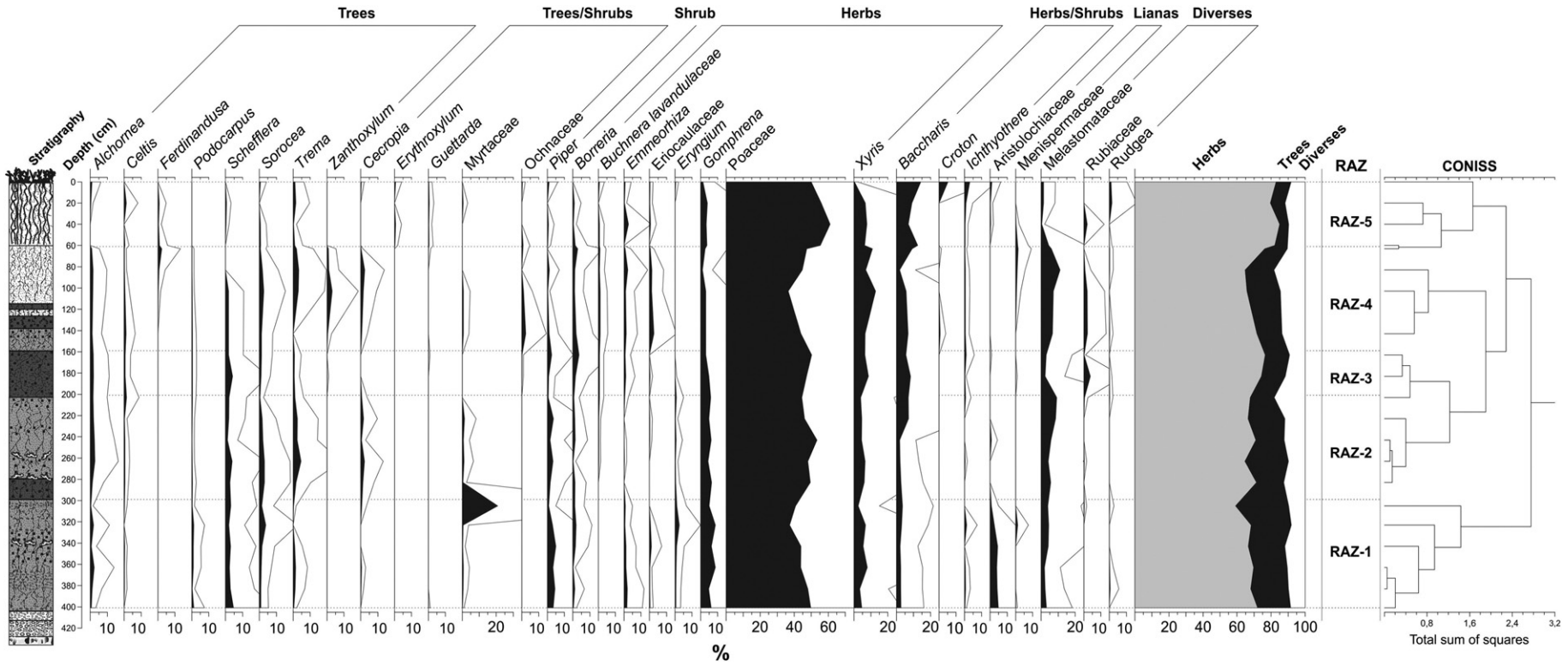

Fig. 4. Synthetic regional (total land pollen sum) palynological diagram of the PdF-I core. The filled silhouettes show the percentage curves of the taxa, while the open silhouettes show the 5X exaggeration curves. CONISS cluster analysis together with the Regional Palynological Zones (RPZ) are plotted. Values of trees, trees/shrubs, shrubs, herbs, herbs/shrubs, lianas and diverse are expressed as percentages of the total land pollen sum.

(*Cerrado lato sensu*). The savanna also contains forested and shrubs formations (*Cerradão*).

3.1.1. Regional signal

Constrained cluster analysis enabled to identify five regional pollen zones (RPZ; Fig. 4 and Supplementary Fig. A.1), while principal components analysis resulted in three components explaining almost 80% of the total variance. The percentage of the variance explained by each principal component was: 38.6% by PC1R, 26.9% by PC2R and 14.2% by PC3R. Pollen zones agree well with the record of the components obtained with PCA and also with major stratigraphic units (Fig. 5). Fractionation of communalities and the factor scores are presented in Figs. 5 and 6.

From 401 to 298 cm, corresponding to zone RPZ-1, the first regional principal component (PC1R) is dominant, explaining 56–80% of variance (Fig. 5) of samples pollen composition. *Schefflera*, Myrtaceae, *Piper*, *Eryngium*, Aristolochiaceae and Melastomataceae pollen types show the largest statistical association to this zone, showing the largest positive factor scores (scores > 1.0; Fig. 6). They are all pioneer species and hygrophytes representatives of semi-deciduous forests, except *Eryngium*, a herbaceous type typical of wet grasslands (Supplementary Table A.1). Myrtaceae shows the highest percentage at the end of this zone (303 cm; Fig. 4). *Podocarpus*, also with highest percentages in RPZ-1, but moderate abundance (score 0.5–1.0; Fig. 6), is a tropical coniferous related to mountainous and cold conditions; these conditions are also supported by the presence of other mountain forest taxa like *Alnus*, *Drimys*, *Mimosa scabrella*, *Weinmannia* and *Myrsine* (Supplementary Fig. A.1). *Alnus* is native from Andes and its presence at the beginning of the zone (Supplementary Fig. A.1) may indicate a long distance transport by winds from the west. Thus, climatic conditions in RPZ-1 were wet and cold.

In RPZ-2 (298–202 cm) PC1R still explains most of the variance indicating the persistence of the semi-deciduous forests, although with moderate decrease to 41% (Fig. 5), and represented by *Trema*, Melastomataceae, *Alchornea* and *Sorocea* (Fig. 6). A succession of pioneering hygrophytes is evident, probably after some disturbance in the environment. At the same time the contribution of second regional principal component (PC2R) increases significantly (up to 36%; Fig. 5), with large to moderate abundances (positive scores) of pollen types of dry savanna, such as *Borreria*, *Zanthoxylum*, Ochnaceae, *Celtis*, Rubiaceae, *Cecropia* and *Buchnera lavandulacea* (Fig. 6). In general, this zone shows conditions that started to diversify, with a gradual replacement of vegetation. A trend to opening of the semi-deciduous and mountain forests was followed by a more characteristic savanna vegetation, in a progressive way.

RPZ-3 (202–158 cm) mostly represents the consolidation of the trends developed in RPZ-2 (Fig. 5). The remnants of semi-deciduous and mountain forests and the wet grasslands were probably located near water courses, while a more or less sparse savanna vegetation covered the area. RPZ-3 represents a change from forest vegetation of humid and cold conditions to one indicating a drier and warmer climate.

RPZ-4 (158–60 cm) shows a definitive decrease in PC1R (to 0.8%) and its substitution by PC2R which attains its maximum contribution in the record (up to 72%; Fig. 5). The expansion of the savanna peaked while semi-deciduous and mountain forests showed the lowest abundances of the record, indicating the highest levels of regional aridity. Climatic conditions in RPZ-4 seem to have been drier and warmer, but often interrupted by short periods of cooling — as the occurrence of taxa characteristic of very cold conditions (i.e. *Alnus*, *Anadenathera*, *Drimys*, *Weinmannia* and *Myrsine*; Supplementary Fig. A.1) indicates.

RPZ-5 (<60 cm) is characterized by large contributions of the third regional principal component (PC3R, up to 52%), a decrease in PC2R (to 1.4%), and minimum, although slightly higher than in RPZ-4, contributions of PC1R (3–10%) (Fig. 5). The PC3R shows larger abundances of pollen types of humid savanna (*Guettarda*, *Ferdinandusa*, *Erythroxylum*, *Croton*, Menispermaceae and *Rudgea*), semi-deciduous forest (Aristolochiaceae), rupicola-saxicolous grassland (Eriocaulaceae and *Xyris*) as well as wet grassland (*Emmeorhiza*; Fig. 6). Some generalist grassland types show large positive factor scores, such as *Baccharis*, *Ichthyothere* and Poaceae (Fig. 6). This heterogeneity of phytophysionomies suggests that the component reflects variations in moisture (humidity) and temperature probably due to well-expressed climate seasonality. With a reduction of savanna vegetation and a small increase in semi-deciduous and mountain forests, conditions of a seasonal and sub-humid climate (as the present one) began to develop. Vegetation cover was more diverse than in the previous pollen zone, being the

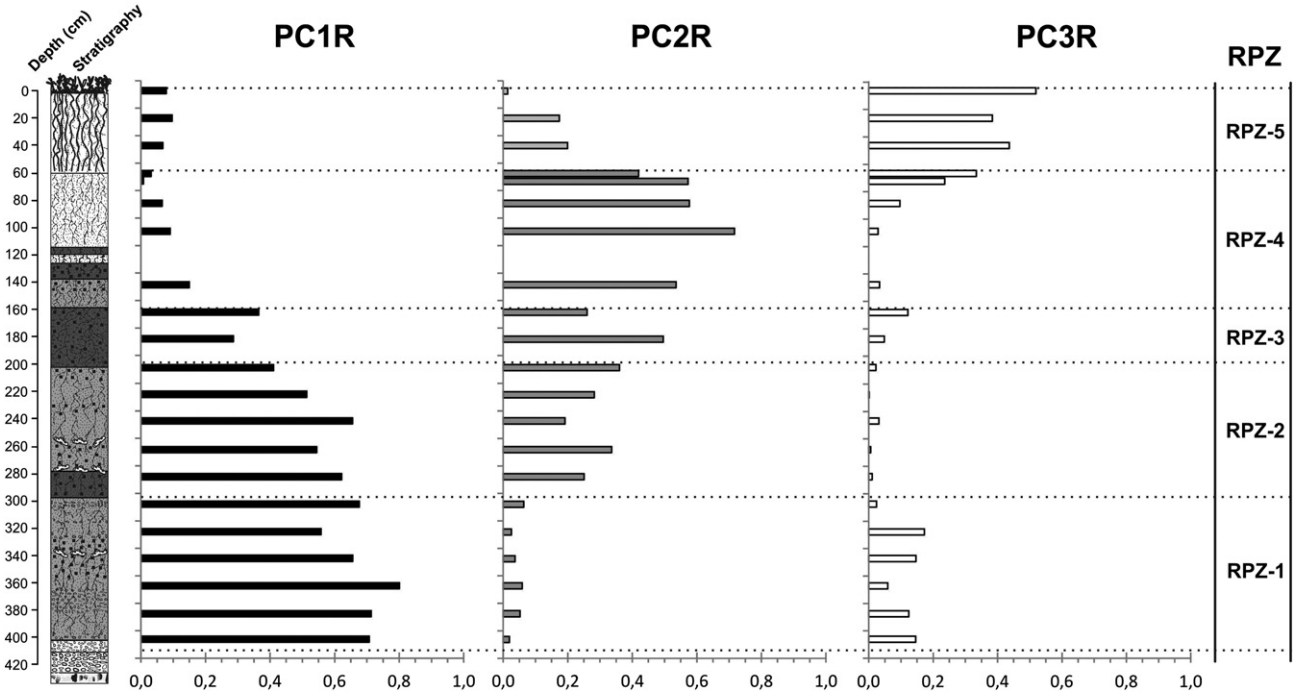

Fig. 5. Squared factor loadings of the three regional (R) PCA components (transposed matrix) explaining the variation of the regional signal of the PdF-I core.

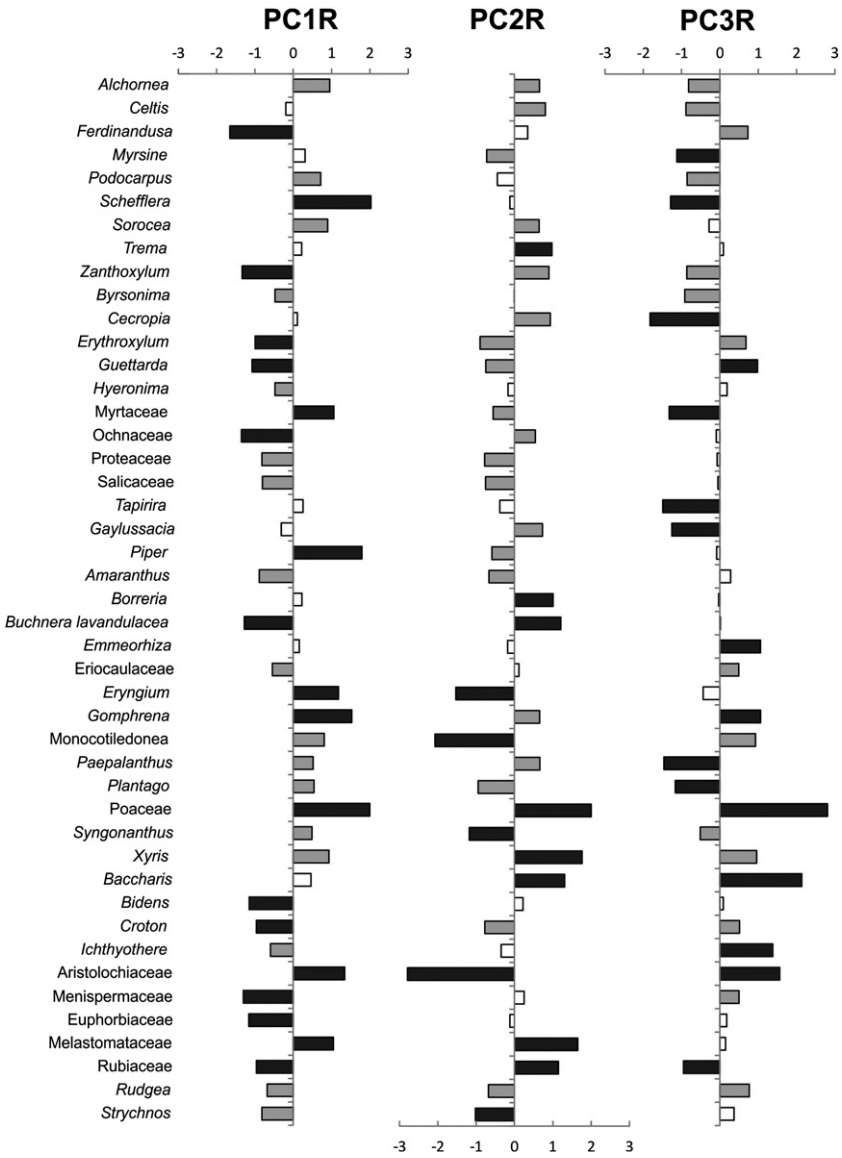

Fig. 6. Factor scores of the pollen types characterizing the three PCA components (transposed matrix) obtained for the regional (R) signal of PdF-I core. Black bars: scores >1.0 or <−1.0, gray bars: scores 0.5–1.0 or −0.5 to −1.0; white bars: scores −0.5–0.5.

rupicola-saxicolous grassland more abundant than the semi-deciduous forests and woody-savanna. Increased humidity and a decrease in temperature are suggested, with conditions similar to present climate.

The PC3R also explained a portion of the variance in RPZ-1 (2.4–17%; Fig. 5). However, even under dominant wet and cold climate (dominance of PC1R), moments with similar current climate possibly existed.

3.1.2. Local signal

Six local pollen zones (LPZ) were detected by constrained cluster analysis (Fig. 7 and Supplementary Fig. A.2), while three principal components explained almost 78% of the total variance. The percentage of the variance explained by each principal component was: 29.5% by PC1L, 26.5% by PC2L and 21.7% by PC3L. The local pollen zones also agree well with the record of the components obtained with PCA and with major stratigraphic units (Fig. 8). Fractionation of communalities and factor scores are presented in Figs. 8 and 9.

In LPZ-1 (401–298 cm) the first local principal component (PC1L) explains most of the variance in the pollen composition of this zone (53–86%; Fig. 8). Hydro-hygrophytes such as Araceae and *Bacopa* and NPP indicators of wet conditions like *Assulina* (van Geel and Middeldorp, 1988; van Geel et al., 1989) and *Meliola niessleana* (fungi parasite on *Calluna*; van Geel, 1976) have large abundances (Fig. 9). The epiphyte/herbaceous *Polypodium*, with moderate abundances (Fig. 9), is indicative of the presence of semi-deciduous forests (Sehnem, 1970), although at present it has also been found in rupicola-saxicolous grassland in the Serra do Espinhaço Meridional (Mendonça et al., 1998; Supplementary Table A.2). Cyperaceae and *Achyrocline* may appear under diverse humidity conditions (Supplementary Table A.1). Low abundances (negative scores) are suggested for *Gelasinospora*, a fungi indicating dry and oligotrophic conditions (van Geel, 1976), and the fern *Notholaena* which is typical of warm, arid to semi-arid conditions (Nobel, 1978). Thus, local conditions in LPZ-1 were wet, and probably cold.

From 298 to 158 cm, corresponding to zones LPZ-2 and LPZ-3, PC1L is substituted by a large increase in the third local principal component (PC3L; up to 73%; Fig. 8). PC3L shows larger abundances of types and NPP pointing to variable humidity/shallow open water conditions (Araceae, *Mougeottia*, *Sellaginella* and *Debarya*; Ellis and van Geel, 1978; Fig. 9), open, disturbed (*Pteridium*) and altered environments (*Pityrogramma trifoliata*; Sánchez-González et al., 2010). *Debarya* has also been described as an airbone algae (Kołaczek et al., 2012), and probably related to greater activity of the monsoon system. *Bacopa*,

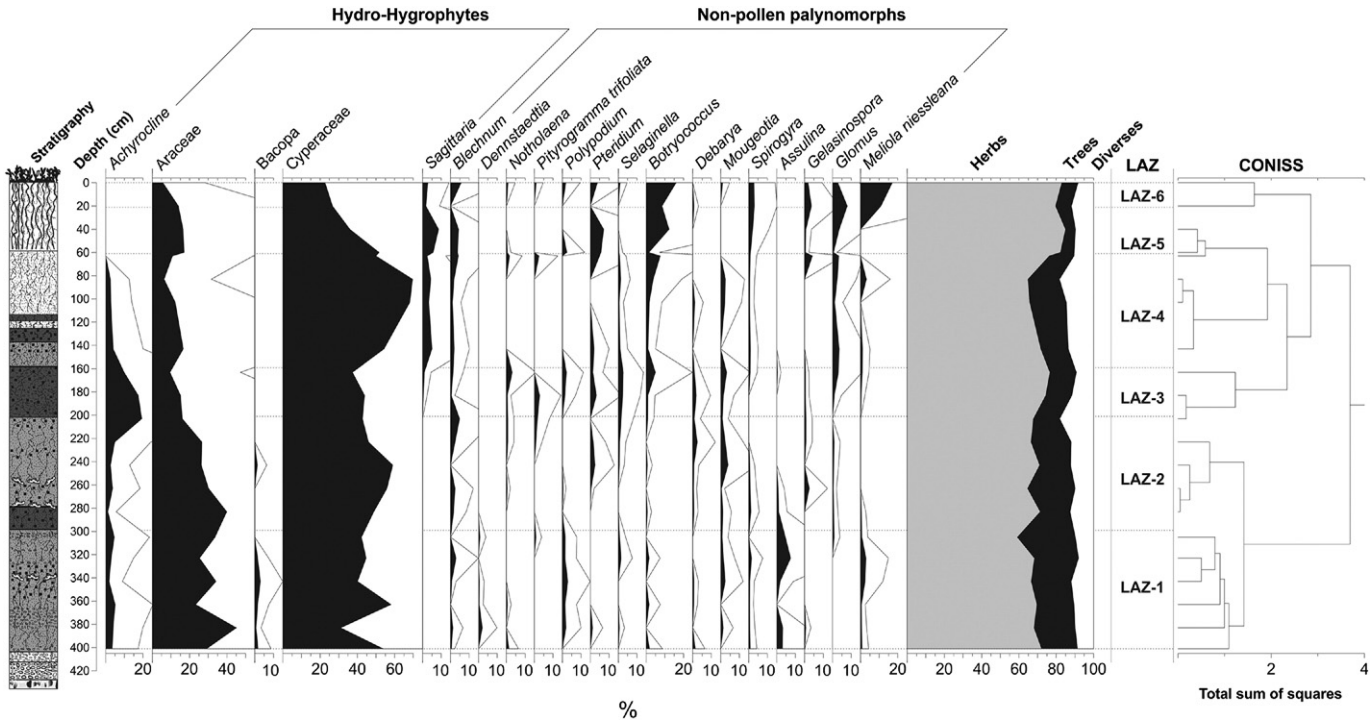

Fig. 7. Synthetic local (hydro-hygrophytes and NPP) palynological diagram of the PdF-I core. The filled silhouettes show the percentage curves of the taxa, while the open silhouettes show the 5X exaggeration curves. CONISS cluster analysis together with the Local Palynological Zones (LPZ) are plotted. Values of hydro-hygrophytes and NPP are expressed as percentages of the total land pollen sum.

Spyrogira, *Assulina* and *Meliola niessleana*, indicators of wet conditions, were low (negative scores; Fig. 9). This assemblage of polen types and NPP reflect in LPZ-2 and LPZ-3 limited, variable, humid conditions, an open and disturbed forest landscape. Conditions seem to have started to diversify more readily at local scale than at regional scale.

From the end of the LPZ-3 to surface, including LPZ-4 (158–60 cm), LPZ-5 (60–20 cm) and LPZ-6 (20–0 cm), PC3L is substituted by a large increase in the second local principal component (PC2L), which becomes dominant (up to 82%) in LPZ-5 (Fig. 8). Larger abundances of types representative of wet grassland (Araceae and *Sagittaria*), plants as *Calluna* (NPP fungi *Meliola niessleana*) and the algae *Spirogyra* and *Botryococcus* are seen in PC2L (Fig. 9), which suggest wet but changing hydrological conditions (Guy-Ohlson, 1992). The positive scores of the fungi *Glomus* and the fern *Blechnum* point to hydric soil erosion (van

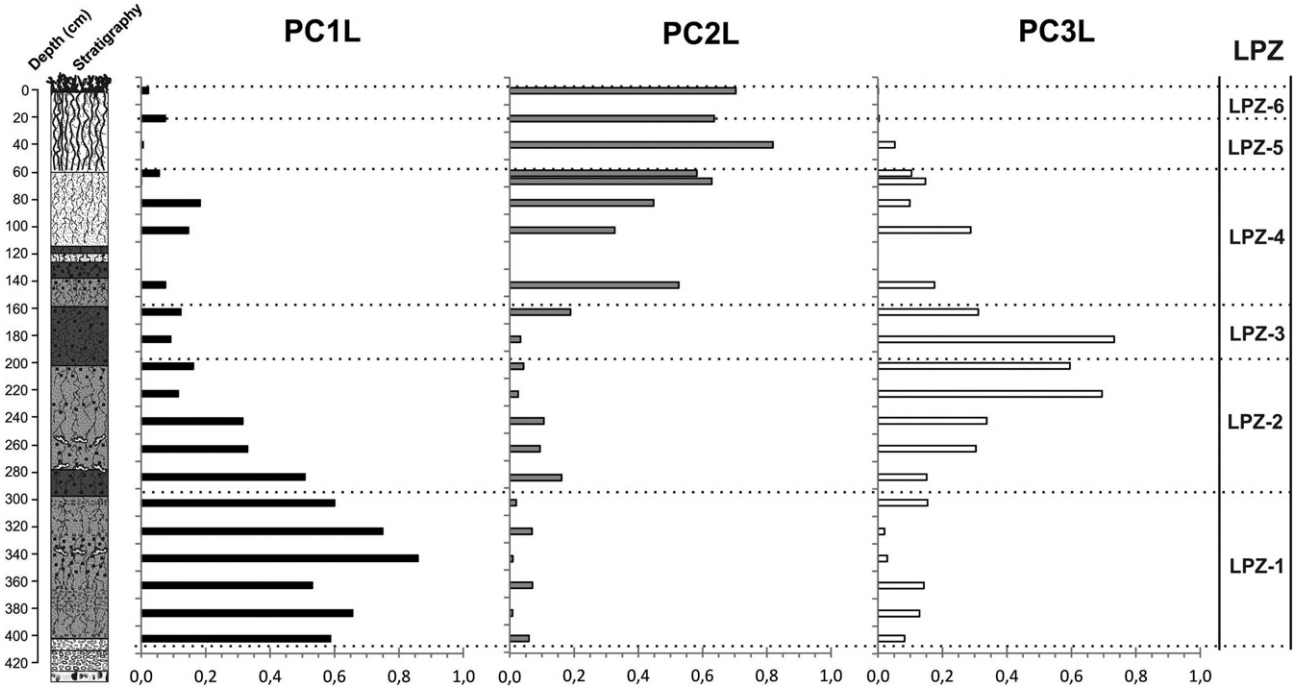

Fig. 8. Squared factor loadings of the three local (L) PCA components (transposed matrix) explaining the variation of the local signal of the PdF-I core.

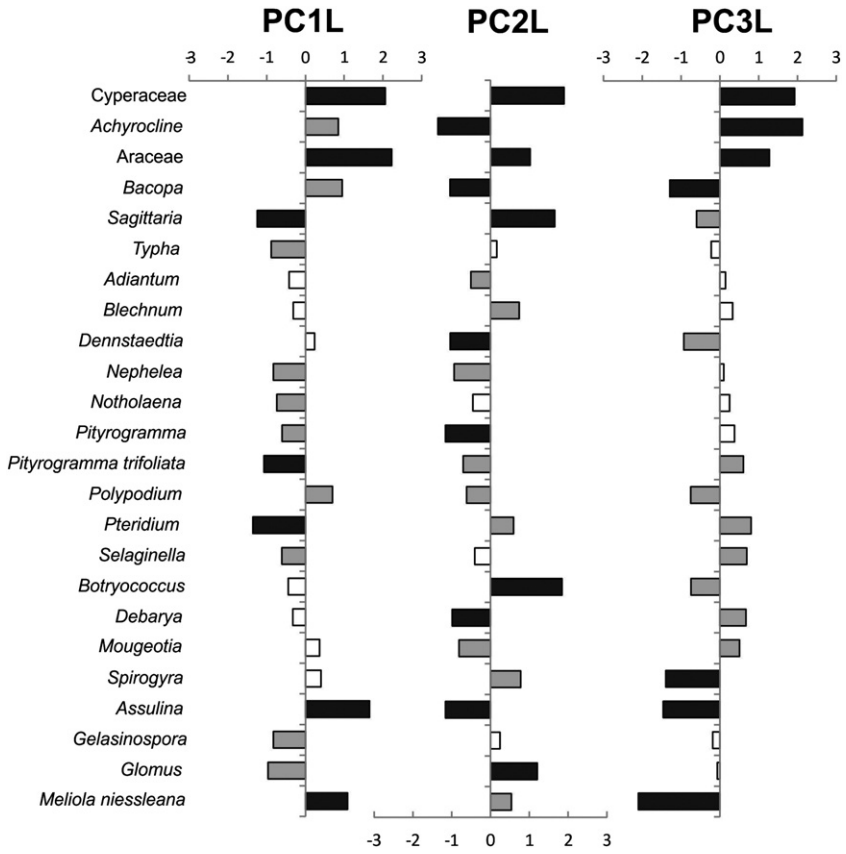

Fig. 9. Factor scores of the pollen types and NPP characterizing the three PCA components (transposed matrix) obtained for the local (L) signal of PdF-I core. Black bars: scores >1.0 or <−1.0, gray bars: scores 0.5–1.0 or −0.5 to −1.0; white bars: scores −0.5–0.5.

Geel and Aptroot, 2006). Landscape disturbance is also indicated by *Pteridium*, a fern usually found in ecological successions of degradation stages (Elliot et al., 1998 observed particularly after fires). Low abundances (negative scores) of *Bacopa*, the fern *Dennstaedtia* and the fungi *Assulina*, all indicators of wet conditions, were also found. The component PC2L reflects local perturbations, with pervasive hydrological changes and soil erosion. In LPZ-5 the highest level of hydrological disturbance is detected. LPZ-6 is characterized by the total disappearance of PC3L and dominance of PC2L (Fig. 8).

3.2. Geochemical composition of the peat

The records of physico-chemical properties and the analyzed elements are provided in the supporting information (Supplementary Figs. B.1, B.2 and B.3). However, selected physico-chemical properties (Ash, BD — bulk density, fiber, C, $\delta^{13}C$ and $\delta^{15}N$) are shown in Fig. 12. Four components explain 80% of the total variance of the geochemical composition of the peat (Table 2). The first component, GC1, explains 43% showing C, N, Cl, Br, Ca, P, Rb and Sr had high positive loadings (>0.7), S, Ti and K had moderate positive loadings (0.5–0.7), and ash content, Si and bulk density (BD) had large negative loadings (Table 2). Most of the elements with positive loadings are biophilic (C, N, S, P, Ca, K) or organically bound (Cl and Br; Biester et al., 2006) elements and are likely to be dependent on the total organic matter content of the peat. While Si, Ti, Rb and Sr are elements hosted by inorganic mineral phases and can thus be taken as indicative of the content of mineral matter; as it is also the case for the ash content and the BD. In contrast to what has been found in other peat records (see for example Weiss et al., 2002), the loadings of these elements indicate that concentrations of Ti, Rb and Sr increase with increasing content of organic matter and decreasing Si, ash and BD. Since the geological material of the catchment of the mire is quartzite, Si contents are most probably related to the amount of quartz transported from the catchment soils to the mire. At the same time, quartz is a mineral highly resistant to weathering that tends to concentrate in the sand fractions, while the other elements (Ti, Rb, Sr) usually concentrate in finer grain sizes (Schuetz, 1989), Ti in particular (Taboada

Table 2
Factor loadings for the four components extracted by PCA using the geochemical composition of the samples of the PdF-I core. Eigenv: eigenvalues; Var (%): percentage of explained variance; BD: Bulk density.

	GC1	GC2	GC3	GC4
N	0.93	0.25		
C	0.92	0.27		
Cl	0.80			
Br	0.80			0.32
Ca	0.79	0.41		
P	0.77	0.31	−0.42	
Rb	0.76	0.42		
Sr	0.70	0.59		
S	0.69	0.26		−0.56
Ti	0.69	0.63		
K	0.68	0.65		
Ash	−0.88			
Si	−0.88			
BD	−0.95			
Zr		0.88		
Al		0.85		
Y	0.49	0.77		
Nb	0.49	0.65		
Fe	0.27		0.93	
Mn			0.89	
Ni			0.80	
Cr	−0.53		0.77	
$\delta^{13}C$		0.37		0.75
$\delta^{15}N$	−0.59			0.69
Eigenv	10.3	4.5	3.1	1.5
Var (%)	43	19	13	6

et al., 2006). Thus GC1 is likely to reflect a local signal: under stable conditions in the catchment the mire accumulated organic matter and soil dust of finer particle size, while under unstable conditions larger amounts of coarse mineral matter (i.e. quartz from the quartzite) were transported to the mire producing an increase in ash content, BD and a relative dilution of both OM and other minerals. Although GC1 is not the main factor controlling their contents in the peat, Y and Nb also have a significant proportion of their variance (24%; Fig. 10) associated to GC1, supporting the interpretation of the physical fractionation effect (both have positive loadings and tend to be enriched in the finer fractions).

The second component, GC2, explains 19% of the variance, showing large positive loadings for Zr, Al, and Y, and a moderate one for Nb (Table 2). Some of the elements (K, Ti, Sr, Rb, Ca) dominated by GC1 have part of their variance in GC2 (Fig. 10). They are also characteristic of the mineral matter of the peat. Zirconium and Al variance is only associated to GC2 and, since GC1 is interpreted as a local signal, it is likely that they reflect the deposition of mineral dust after longer transport. i.e. a regional dust signal. Except for Zr and Al, the PCA results suggest that the other elements have at least two different sources (local and regional). This is supported by the fact that the (K, Ti, Sr, Rb, Ca)/Zr ratios (not shown) are strongly correlated to GC1 scores (Pearson correlation coefficient, r 0.73–0.83) while the Al/Zr ratio is not correlated (r −0.11). Since quartzites have low concentrations of the elements characteristic of GC2 and the closest geological materials surrounding the Sopa-Bramadinho formation, with potentially larger concentrations of these elements, are located 40–50 km W and E of the mire (Fig. 1), GC2 may represent the deposition of regional dust after, at least, some tens of kilometers of atmospheric transport.

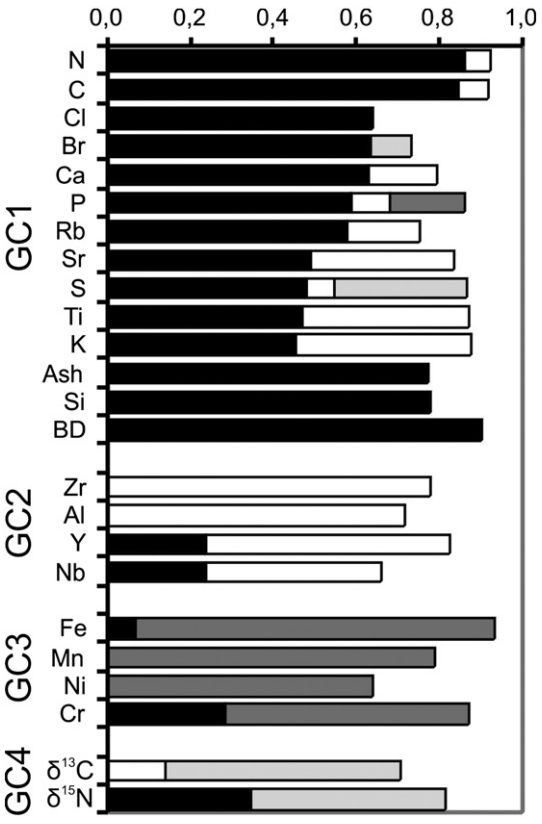

Fig. 10. Fractionation of communalities of the variables used in the PCA of geochemical properties of the peat of PdF-I core. The communality of each variable (i.e. the proportion of its variance explained by each component) corresponds to the total length of the bar; the sections of the bars represent the proportion of variance in each component. The variables are ordered by the component with the largest share of variance.

The third component, GC3, explains 13% of the variance and some metals (Fe, Mn, Ni, Cr) are the elements showing large positive loadings (Table 2). Most of the elements in this component have a marked redox behavior (see for example Chesworth et al. 2006) and, as it will be discussed later, their co-occurrence in the same peat sections may reflect co-precipitation after being remobilized under anoxic conditions. But Cr also shows a significant proportion of its variance (29%; Fig. 10) associated to GC1, the negative loading indicating that its concentration tends to increase with the increase in quartz and, possibly, coarse mineral matter in the peat, pointing to a catchment source.

The fourth component, GC4, explains 6% of the variance and is represented by the isotopic signature of the organic matter ($\delta^{13}C$ and $\delta^{15}N$) (Table 2). The isotopic ratios also have a significant proportion of their variance in another component: $\delta^{15}N$ has a 35% in GC1 (Fig. 10), its negative loading suggesting that the ratio is higher in layers containing higher amounts of coarse mineral matter and lower in peat sections rich in organic matter; while $\delta^{13}C$ has a 14% of variance in GC2 (Fig. 10), indicating that slightly heavier isotopic compositions are found in samples with higher contents of mineral matter originated from regional dust deposition. For the $\delta^{15}N$ the correlation to GC1 scores is highly significant (r 0.75) if the upper peat layer (<60 cm) is excluded. Thus, GC4 accounts for the shared signal of both isotopic ratios and probably reflects the co-variation in the samples contributing to most of the variance (that of the mineral sediment and those of the upper peat section).

As it can be seen in Fig. 11 the changes in GC1 scores show a good agreement with the stratigraphy of PdF-I core. The lowest scores are found at the base of the core and correspond to the mineral sediment. The first organic rich horizon (Oa7, 404–298 cm; Fig. 1) shows an increase in GC1 scores, although the still negative values indicate a predominance of mineral matter (as also supported by the high ash content and bulk density and the low content in fiber, Fig. 12). The average C content of this horizon (6.1 ± 2.6%) is exceeded at its base and a peak at 338–348 cm, reaching up to 10.3% (Fig. 12). At 298 cm the scores increase abruptly and remain positive until 198 cm indicating the accumulation of minerogenic peat and an important decrease in the flux of mineral matter from the catchment. From 198 to 158 cm the scores decrease again to negative values pointing to an increase in the mineral content (mainly quartz), with values similar to those of the first organic horizon (404–298 cm). By 158 cm the scores increase to moderate positive values until 119 cm, corresponding to the start of a second phase of peat accumulation. After that scores increase sharply to remain stable, at maximum values, until 60 cm; being this section the one with the largest C contents (Fig. 12). The upper 60 cm shows lower, but still positive, almost constant scores.

GC2 scores also show agreement with the stratigraphy (Fig. 11). Negative scores, indicative of low contributions of regional dust, are generally found below 298 cm, except for a peak at 338–348 cm. The scores remain positive, with small variations, from 298 to 119 cm. At 119 cm they decrease abruptly coinciding with the largest values of GC1 scores and suggesting a decrease in the dust flux (local and regional) to the mire. The flux of regional dust recovers in the upper peat section (<60 cm).

The content of metals in GC3 is highly irregular below 298 cm; shows elevated values between 278 and 230 cm, and generally low values in the upper 230 cm (Fig. 11). Discrete peaks are found at 388, 348, 210, 158 and 58 cm. Elevated metal concentrations were found in peat sections formed under wetter climate conditions (corresponding to cold periods in the North Atlantic represented in Fig. 13; Bond et al., 2001, as it is discussed below) suggesting that changing redox conditions linked to variations in water table depth may have been responsible for their remobilization and precipitation.

The isotopic signature of the organic matter captured by GC4 shows high scores at the base of the core and in the upper peat sections (Fig. 11). The $\delta^{13}C$ ratios of the upper peat section (Fig. 12) point to a rapid shift from C3 to C4 vegetation. Small variations are observed in the rest of the record, with relatively lower values between 398–220 cm and 119–60 cm, and relatively higher between 210 and 130 cm.

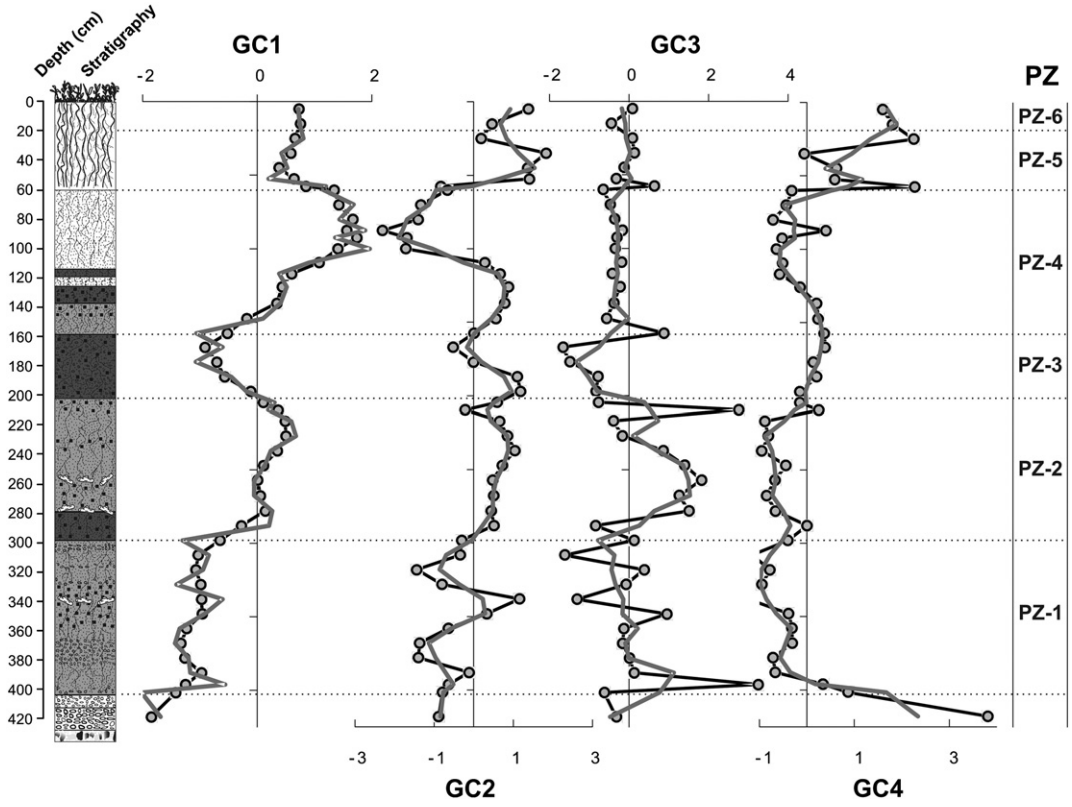

Fig. 11. Record of factor scores of the four principal components extracted for the geochemical composition of the PdF-I core and Palynological Zones (PZ).

4. Discussion

4.1. Chronology of the changes

Some selected proxies are represented in Fig. 13 to synthesize the chronology of the changes occurred during the Holocene in the Serra do Espinhaço Meridional. The figure also contains the record of hematite-stained grains (HSG) of the North Atlantic (Bond et al., 2001), which reflects variations in temperature at high northern latitudes. HSG variations were found to match the changes in oxygen isotopic composition of a speleothem collected from Lapa Grande cave (Stríkis et al., 2011), located at the north of the Minas Gerais State — some 400 km north of Pau de Fruta mire. Increased contents of HSG are related to colder temperatures in the North Atlantic and wetter

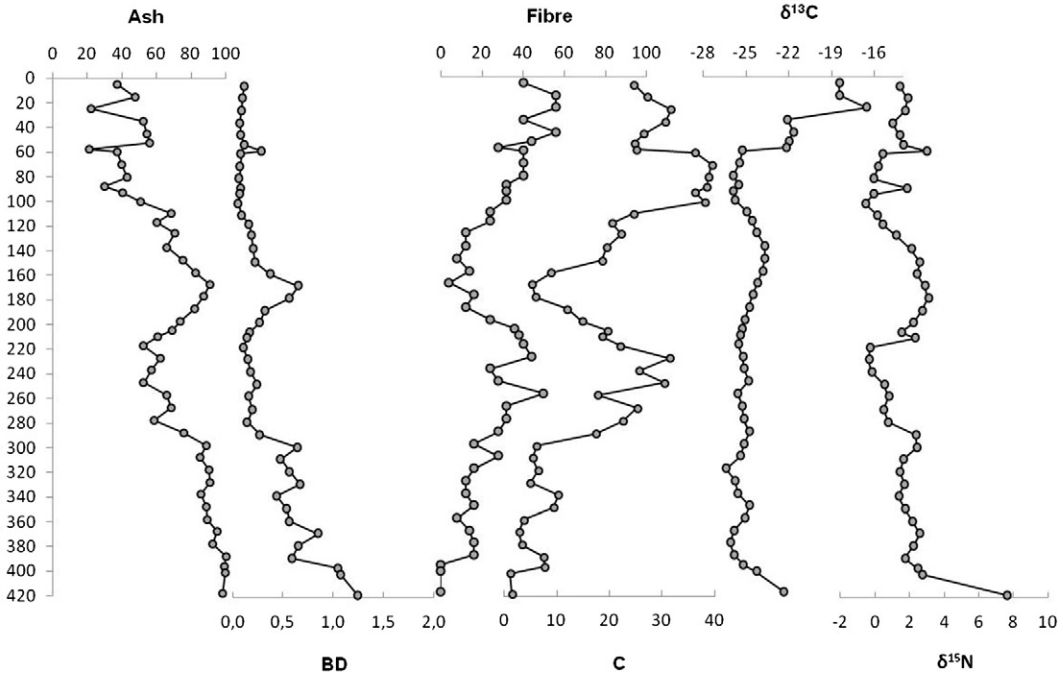

Fig. 12. Contents (in %) of ash, fiber and C; BD (in Mg m^{-3}); and $\delta^{13}C$ and $\delta^{15}N$ (in ‰) of the PdF-I core.

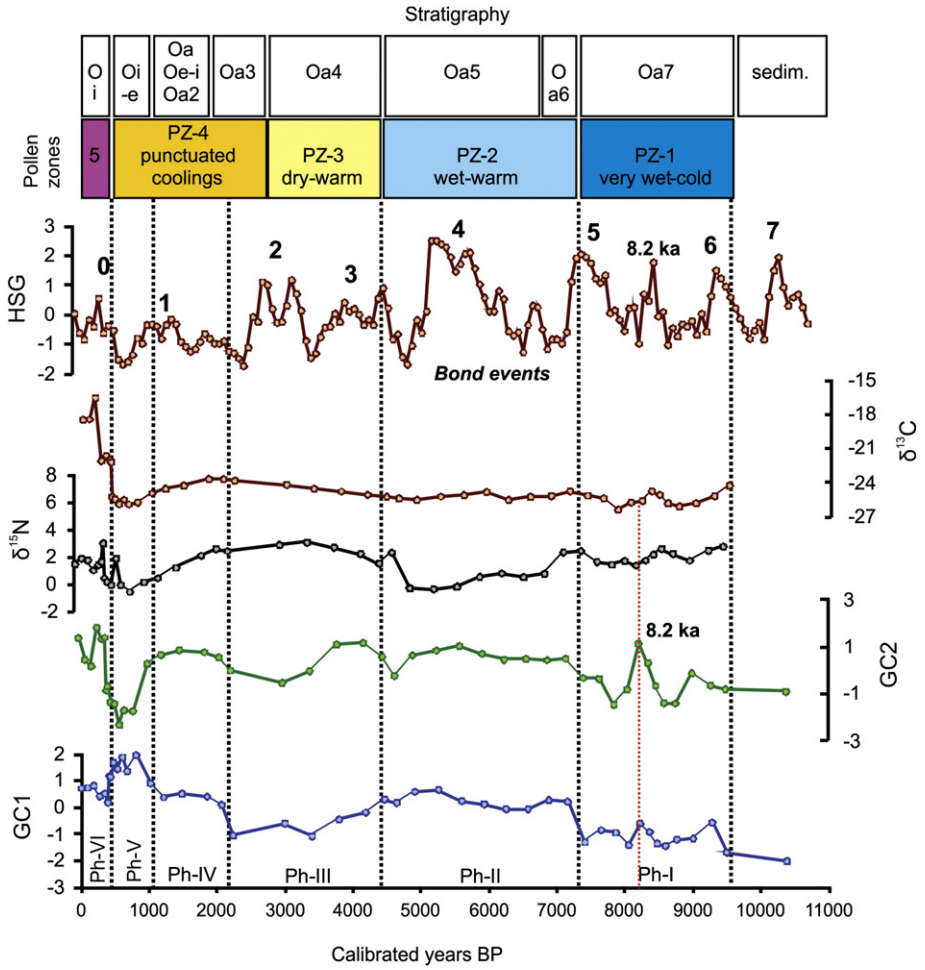

Fig. 13. Chronology of Holocene environmental changes recorded in the Pau de Fruta mire. GC1 and GC2: scores of the two first geochemical components extracted with PCA; HSG: standardized values of the N Atlantic hematite-stained grains record (original data obtained from Bond et al., 2001). $\delta^{13}C$ and $\delta^{15}N$ in ‰. Dark blue: very wet; light blue: wet; yellow: dry; orange: very dry; purple: sub-humid climatic.

conditions in central–eastern Brazil. Thus, the HSG record is used here as a context for the inferred climate changes of our study. The combination of proxies enables to define six main phases of change.

Phase I (~10,000–7360 cal. yr BP, horizon Oa7) represents the start of organic matter accumulation at the beginning of the Holocene (by ~9500 cal. yr BP). This horizon has a high content in inorganic matter and its geochemical composition indicates a dominance of inputs from the mire's catchment, suggesting landscape instability. A large increase in GC2 scores (possible regional dust deposition, Fig. 13) occurred by ~8200–8300 cal. yr BP, which coincides with the 8.2 ka event, and suggests changing conditions for atmospheric transport (stronger winds, a change in wind frequency or direction, greater availability of source areas, or a combination of factors). The vegetation was dominated by dense semi-deciduous and mountain forests and wet rupicola-saxicolous grasslands, indicating very wet and cold climate conditions. The start of this phase is coeval with Bond event 6 and its termination with the abrupt end of Bond event 5 (Fig. 13). The start of organic matter accumulation may have been triggered by the increase in humidity in the early Holocene.

Phase II (~7360–4200 cal. yr BP, horizons Oa6 and Oa5) shows a sharp increase in organic matter content, a decrease in the local fluxes of inorganic matter and a relative, almost constant, dominance of the regional dust component (with the exception of a local decrease by ~4600 cal. yr BP, Fig. 13). A decline in mountain forests and the opening of the semi-deciduous forests with expansion of savanna formations suggest warmer conditions and a certain decrease in humidity; however, the conditions remained to be wet. The abrupt end of Bond event 5 and development of relatively drier conditions agree well with the formation of the highly sapric (i.e. highly decomposed peat) Oa6 horizon.

Phase III (~4200–2200 cal. yr BP, horizons Oa4 and Oa3) is characterized by a large increase in the flux mineral matter from the catchment, surely related to severe soil erosion, with contents comparable to those of horizon Oa7 of phase I (reaching up to 90%, see Fig. 12). Between ~4200 and 3800 cal. yr BP the contribution of regional dust was significant, but after ~3800 cal. yr BP the local signal overrode the regional one and the mire evolved to conditions similar to those of the early Holocene. The vegetation showed a decline of semi-deciduous forests and expansion of formations typical of drier conditions. At a local level, perturbations of the catchment hydrology are suggested, their intensity being reduced by the end of the phase. The decrease in humidity may have been accompanied by increased rainfall seasonality and torrentiality, based on a greater diversity of regional pollen types.

Phase IV (~2200–1160 cal. yr BP; horizons Oa2, Oe-i, and Oa) shows a recovery to geochemical conditions similar to those of phase II (Fig. 13), pointing to a decrease in local soil erosion and increase in regional dust deposition. Vegetation was still dominated by savanna formations under dry conditions, although periods of punctuated cooling, possibility also accompanied by variations in humidity, are suggested. This is supported by more frequent changes in peat stratigraphy.

Phase V (~1160–400 cal. yr BP, horizon Oi-e) shows the largest increase in organic matter accumulation and a sharp reduction in local and regional fluxes of mineral matter (Fig. 13), suggesting environmental stability in both the catchment and at regional scale.

Phase VI (< ~400 cal. yr BP, horizon Oi) represents an abrupt shift. At the beginning of the phase there is a sudden increase in the regional dust signal (the largest of the whole record), together with a moderate increase in the local flux of mineral matter (comparable to phases IV and II). The C isotopic composition also shows an abrupt change to values typical of C4 plants, while the regional and local pollen indicators recorded large hydrological disturbances and soil erosion, but also a certain increase in humidity in the last couple of centuries (as indicated by the slight recover of the humid forests).

The phases determined and environmental conditions inferred from the PdF-I record agree well with paleoclimatic interpretations obtained from other peat, lake sediments and speleothem records in central Brazil. Cold and humid conditions, as those proposed for phase I in Pau de Fruta, were verified in the isotopic record of Lapa Grande (Stríkis et al., 2011). Cold conditions were also suggested for the period 10,360–8840 cal. yr BP in the Salitre peat record (Ledru, 1993), reflected by the presence of *Araucaria* forests. Wet conditions are supported by the predominance of semi-deciduous forests in the record of Lagoa Nova between ca. 9540 and 8220 cal. yr BP (Behling, 2003), and by the expansion of the gallery forest in Lago do Pires between ca. 9910 and 8180 cal. yr BP (Behling, 1995a). In the later record, the decrease in the abundance of mountain forest suggests slightly warmer conditions than those of the Bond event 6. A shift to wetter conditions is also recorded in Lapa Grande (Stríkis et al., 2011) during the 8.2 ka event and Bond event 5.

In phase II the PdF-I record points to a decrease in humidity. In the Lagoa Nova record there is an expansion of *Cerrado* formations and regression of the gallery forest between ca. 7560 and 6060 cal. yr BP; a sharp decrease in tree pollen and NPP indicators of wet environments between ca. 6320 and 4875 cal. yr BP was found in the Salitre record; and drawdowns in lake level with development of a fen phase were found in Lagoa dos Olhos ca. 7865–7415 cal. yr BP (De Oliveira, 1992), and Lagoa Santa between 7165 and 5590 cal. yr BP (Parizzi et al, 1998). In Lagoa da Serra Negra, apart from a reduction in humidity (expansion of *Cerrado* formations and retreat of semi-deciduous forests), increased temperatures are suggested after 5900–5580 cal. yr BP. Phase II also coincides with the start of the so called "Archaic Gap" (Araujo et al., 2005) in the state of Minas Gerais, a phase of abandonment of settlements and depopulation that was related to the onset of arid conditions. In PdF-I the peat section coeval with Bond event 4 is represented by a slight increase in humidity and warmer temperatures than in previous events.

The second half of the "Archaic Gap" period corresponds to phase III of the PdF-I record. Climate was probably more arid and warmer than in the previous phase, as supported by the low abundances or absence of pollen types characteristic of forests and humid grasslands and the increase in savanna types. A similar situation was inferred in Lagoa Nova ca. 2950–2790 cal. yr BP, from the dominance of *Cerrado* (savanna) and *Cerradão* (tree-shrub savanna) formations. Despite the general arid conditions, in PdF-I two periods of increased humidity coincided with Bond events 3 and 2. Higher humidity was interpreted in the Salitre record between 4750 and 3350 cal. yr BP based on increased abundance of the semi-deciduous forest, and by the formation of the lake in Lagoa dos Olhos by ca. 4350 cal. yr BP. The second humid pulse was recorded after ca. 3350 cal. yr BP in Lagoa Santa, reflected by a mosaic of forest and *Cerrado* formations – under a sub-humid climate.

In phase IV maximum aridity is suggested by the pollen record of PdF-I, with the largest expansion of *Cerradão*, similar to what has been reconstructed in Lagoa Nova for the same period. Nevertheless, conditions seem not to have been constant as increased humidity and cooling periods, particularly during the timing of Bond event 1, were also inferred. From 1270–970 cal. yr BP in Lagoa da Serra Negra, 1320–1050 cal. yr BP in Lagoa dos Olhos and ca. 1400 cal. yr BP in Lagoa Santa – close to Bond event 1 – humidity approached that at present indicating a relative increase.

No record exists for phase V in Lagoa da Serra Negra and Salitre, due to the presence of hiatuses. In Lagoa Nova arid conditions, represented by *Cerradão* formations, continued until 600 cal. yr BP.

The start of phase VI occurred about a century after the arrival of Portuguese to Brazil and coincides with the initiation of gold mining activities (Machado and Figueirôa, 2001). The 17th and 18th centuries CE were known as the "gold cycle". In 1714 CE the first diamonds were found close to the Diamantina city (the origin of its name) and the Pau de Fruta mire. Mining intensity decreased with time but some activity persisted until today. Since the 18th century CE population has increased abruptly, several roads were built around the mire, deforestation became extensive, and in 1927 CE a water reservoir for the Diamantina city was constructed at the outlet of the mire. This increased human impact in the landscape may have been responsible for the abrupt change indicated by the PdF-I record in phase VI. Despite the enhanced anthropization of landscape, climate also showed significant changes during this period (as the Little Ice Age), which may have contributed to the abrupt shift from a C3 to a dominant C4 vegetation (Fig. 13) in the Pau de Fruta mire.

4.2. Mire's behavior in phase space

Following Dearing (2008), the evolution of Pau de Fruta mire (its system behavior) can be examined using a phase space diagram (i.e. "*a bivariate plot showing the temporal sequence of points*"). In Fig. 14 we have represented the GC1–GC2 projection, that is assumed to show the combination of local (GC1) and regional (GC2) signals based on the geochemical composition of the peat/sediments of the PdF-I core. Three main states are suggested, the first one (S1) represented by the early Holocene (phase I, ~10,000–7360 cal. yr BP), indicating catchment instability with large fluxes of local mineral matter and a low contribution of regional dust. The second state (S2) occurs under increased stability in the catchment, with lower fluxes of local mineral matter and enhanced deposition of regional dust. On the other hand, the third state (S3) represents highly stable local and regional conditions and the largest accumulation of organic matter in Pau de Fruta.

The graph shows that changes between states have been rather abrupt, as it also happened during the 8.2 ka event. The main exception is the evolution of phase III, in which the shift from S2 seems to have been preceded by a transition (~4200–3800 cal. yr BP) to conditions

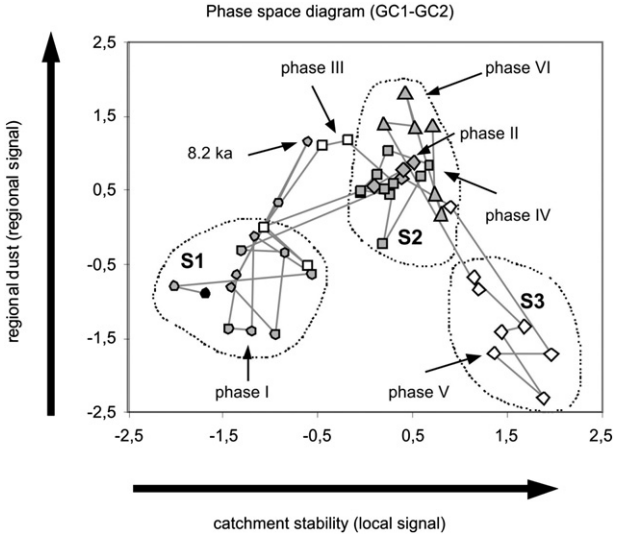

Fig. 14. Phase space diagram of the two first geochemical components, representing local and regional fluxes of mineral matter (i.e. stability) to the Pau de Fruta mire.

similar to those of the 8.2 ka event, before the abrupt change to S1 occurred. S2 and S3 represent stages of peat accumulation and peatland development, while S1 seems to reflect phases of large mineral fluxes from the catchment.

5. Conclusions

The multi-proxy investigation of the Pau de Fruta mire (PdF-I core) suggests that Holocene environmental evolution in central–eastern Brazil was mainly linked to climate change. Peat stratigraphy is the visual evidence we have today of past changes, and it coincided with the variations found in vegetation and landscape dynamics. The combination of proxies enabled us to define six main phases of change: phase I (~10,000–7360 cal. yr BP), II (~7360–4200 cal. yr BP), III (~4200–2200 cal. yr BP), IV (~2200–1160 cal. yr BP), V (~1160–400 cal. yr BP) and VI (<~400 cal. yr BP). The changes in vegetation suggested very wet and cold (phase I), wet and warm (phase II), dry and warm (phase III), and dry and punctuated cooling (phase IV) conditions until the current sub-humid (phases V–VI) climate was set up. Climate changes were accompanied by local (phases I and III) and/or regional (phases II and IV) reactivations of soil erosion. The 8.2 ka event was clearly identified by a large relative increase in GC2 scores possibly representing accelerated regional dust accumulation. Similar conditions to this event were found for the transition from phase II to phase III (4200–3800 cal. yr BP). Reduced local and regional erosion and increased accumulation of organic matter were reconstructed for phase V.

Changes in PdF-I peat stratigraphy and the detected episodes of local erosion were probably related to intense hydrological changes in the mire catchment. But, although climate was the most important driving force of environmental change, human activity seems to have been also involved in the dramatic change occurred over the past 400 years (phase VI). These included mining activities, such as the "gold cycle" during the 17th and 18th centuries CE and the extraction of diamonds since 1714 CE until today; abrupt increase in population, construction of roads around the mire and extensive deforestation since the 18th century CE, and construction of a water reservoir for Diamantina city at the outlet of the mire in 1927 CE.

The temporal sequence of the evolution of the local and regional erosion proxies suggests that the Pau de Fruta mire had three main states reflecting conditions of local landscape instability (in phase I) or stability (in phases II, IV and VI) in the mire catchment; with transitional conditions during the 8.2 ka event and most of phase III. During the phases of stability there was enhanced deposition of regional dusts, except for phase V which reflects the most stable conditions during the Holocene.

Acknowledgments

This work was supported by Fundação de Amparo à Pesquisa do Estado de São Paulo (FAPESP)/Brazil (grant to I.H.T - regular doctoral scholarship FAPESP 2010/51637-0 and research internships abroad BEPE/FAPESP 2012/00676-1), Conselho Nacional de Desenvolvimento Científico e Tecnológico (CNPq)/Brazil (Universal 14/2011 – 482815/2001-6), Ministério de Economia y Competitividad/España (CGL2010-20662) and Xunta de Galícia/España (10PXIB200182PR). We are grateful to Noemí Silva Sánchez, Luiz Rodriguez Lado and Manuela Costa Casais (Univesidad de Santiago de Compostela), Márcia Aguiar de Barros (Universidade Federal do Rio de Janeiro), Fabrício da Silva Terra (Universidade dos Vales do Jequitinhonha e Mucuri) and José Ricardo da Rocha Campos (Universidade Tecnológica Federal do Paraná) for their collaboration and assistance during different stages of the research. We also would like to thank the Companhia de Saneamento de Minas Gerais (COPASA - Pau de Fruta/Diamantina) for enabling accessibility to the study area.

Appendix A. Supplementary data

Supplementary data associated with this article can be found in the online version, at http://dx.doi.org/10.1016/j.palaeo.2015.07.027. These data include the Google map of the most important areas described in this article.

References

Araujo, A.G.M., Neves, W.A., Piló, L.B., Atui, J.P.V., 2005. Holocene dryness and human occupation in Brazil during the "Archaic Gap". Quat. Res. 64, 298–307.
Arz, H.W., Gerhardt, S., Pätzold, J., Röhl, U., 2001. Millennial-scale changes of surface- and deep-water flow in the western tropical Atlantic linked to Northern Hemisphere high-latitude climate during the Holocene. Geology 29, 239–242.
Baker, P.A., Seltzer, G.O., Fritz, S.C., Dunbar, R.B., Grove, M.J., Tapia, P.M., Cross, S.L., Rowe, H.D., Broda, J.P., 2001. The history of South American tropical precipitation for the past 25,000 years. Science 291, 640–643.
Baker, P.A., Fritz, S.C., Garland, J., Ekdahl, E., 2005. Holocene hydrologic variation at Lake Titicaca, Bolivia/Peru, and its relationship to North Atlantic climate variation. J. Quat. Sci. 20, 655–662.
Behling, H., 1995. A high resolution Holocene pollen record from Lago do Pires, SE Brazil: vegetation, climate and fire history. J. Paleolimnol. 14, 253–268.
Behling, H., 2003. Late glacial and Holocene vegetation, climate and fire history inferred from Lagoa Nova in the southeastern Brazilian lownland. Veg. Hist. Archeobotany 12, 263–270.
Biester, H., Martínez Cortizas, A., Keppler, F., 2006. Occurrence and fate of halogens in mires. In: Martini, I.P., Martínez Cortizas, A., Chesworth, W. (Eds.), Peatlands Evolution and Records of Environmental and Climate Changes. Elsevier Series Development in Earth Processes, Netherlands, Oxford, pp. 449–464.
Blaauw, M., 2010. Methods and code for 'classical' age-modelling of radiocarbon sequences. Quat. Geochronol. 5, 512–518.
Bond, G., Kromer, B., Beer, J., Muscheler, R., Evans, M.N., Showers, W., Hoffmann, S., Lotti-Bond, R., Hajdas, I., Bonani, G., 2001. Persistent solar influence on North Atlantic climate during the Holocene. Science 294, 2130–2136.
Booth, R.K., Jackson, S.T., Notaro, M., 2010. Using peatland archives to test paleoclimate hypotheses. In: Jackson, S.T., Charman, D., Newman, L., Kiefer, T. (Eds.), Peatlands: Paleoenvironments and Carbon Dynamics. Past Global Changes, Bern, Switzerland, pp. 6–10.
Campos, J.R.R., 2014. Relationship morphology, stratigraphy and hydrology in the formation of peatlands in the Serra do Espinhaço Meridional (MG) PhD Thesis Escola Superior de Sgricultura Luiz de Queiroz, Universidade de São Paulo, Brasil.
Chambers, F.M., Daniell, J.R.G., Alm, J., Bartlett, S., Begeot, C., Bingham, L., Blaauw, M., Blundell, A., Chambers, F., Charman, D., Daniell, J., Evershed, R., Karofeld, E., Korhola, A., Kuester, H., Laine, J., Magny, M., Mauquoy, D., McClymont, E., Mitchell, F., Oksanen, P., Pancost, R., Sarmaja-Korjonen, K., Seppä, H., Sillasoo, U., Steffanini, B., Steffens, M., Tuittila, E.S., Väliranta, M., van der Plicht, J., van Geel, B., Yeloff, D., 2010. Peatland archives of late-Holocene climate change in northern Europe. In: Jackson, S.T., Charman, D., Newman, L., Kiefer, T. (Eds.), Peatlands: Paleoenvironments and Carbon Dynamics. Past Global Changes, Bern, Switzerland, pp. 4–6.
Cheburkin, A.K., Shotyk, W., 1996. An Energy-dispersive Miniprobe Multielement Analyzer (EMMA) for direct analysis of Pb and other trace elements in peats. Fresenius J. Anal. Chem. 354, 688–691.
Cheng, H., Sinha, A., Cruz, F.W., Wang, X., Lawrence Edwards, R., d'Horta, F.M., Ribas, C.C., Vuille, M., Stott, L.D., Auler, A.S., 2013. Climate change patterns in Amazonia and biodiversity. Nat. Commun. 4 (1411), 1–6.
Chesworth, W., Martínez Cortizas, A., García-Rodeja, E., 2006. The redox–pH approach to the geochemistry of the Earth's land surface, with application to peatlands. In: Martini, I.P., Martínez Cortizas, A., Chesworth, W. (Eds.), Peatlands: Evolution and Records of Environmental and Climate Changes. Elsevier Series Development in Earth Processes, Netherlands, Oxford, pp. 175–195.
Cruz, F.W.J., Burns, S.J., Karmann, I., Sharp, W.D., Vuille, M., Cardoso, A.O., Ferrari, J.A., Dias, P.L.S., Viana, O.J., 2005. Insolation driven changes in atmospheric circulation over the past 116,000 years in subtropical Brazil. Nature 434, 63–66.
Cruz, F.W., Vuille, M., Burns, S.J., Wang, X., Cheng, H., Werner, M., Lawrence Edwards, R., Karmann, I., Auler, A.S., Nguyen, H., 2009. Orbitally driven east–west antiphasing of South American precipitation. Nat. Geosci. 2, 210–214.
Daley, T.J., Mauquoy, D., Chambers, F.M., Street-Perrott, F.A., Hughes, P.D.M., Loader, N.J., Roland, T.P., van Bellen, S., Garcia-Meneses, P., Lewin, S., 2012. Investigating late Holocene variations in hydroclimate and the stable isotope composition of precipitation using southern South American peatlands: an hypothesis. Clim. Past 8, 1457–1471.
De Oliveira, P.E., 1992. A palynological record of Late Quaternary vegetational and climatic change in southeastern Brazil PhD Thesis The Ohio State University Columbus, Ohio.
Dearing, J.A., 2008. Landscape change and resilience theory: a palaeoenvironmental assessment from Yunnan, SW China. The Holocene 18, 117–127.
Deplazes, G., Lückge, A., Peterson, L.C., Timmermann, A., Hamann, Y., Hughen, K.A., Röhl, U., Laj, C., Cane, M.A., Sigman, D.M., 2013. Links between tropical rainfall and North Atlantic climate during the last glacil period. Nat. Geosci. 6, 213–217.
Ekdahl, E.J., Fritz, S.C., Baker, P.A., Risgby, C.A., Coley, K., 2008. Holocene multidecadal- to millennial-scale hydrologic variability on the South American Altiplano. The Holocene 18, 867–876.
Elliot, M.B., Flenley, J.R., Sutton, D.G., 1998. A late Holocene pollen record of deforestation and environmental change from the Lake Tauanui catchment, Northland, New Zealand. J. Paleolimnol. 19, 23–32.

Ellis, A.A.C., van Geel, B., 1978. Fossil zygospores of *Debarya glyptosprema* (De Bary) Wittr. (Zygnemataceae) in Holocene sandy soils. Acta Bot. Neerl. 27, 389–396.
Eriksson, L., Johansson, E., Kettaneh-Wold, N., Wold, S., 1999. Introduction to Multi- and Megavariate Data Analysis Using Projection Methods (PCA & PLS). Umetrics AB, Umea.
FAO (Food and Agriculture Organization), 2006. Guidelines for Soil Description. Management Service, Rome.
Garreaud, R.D., Vuille, M., Compagnucci, R., Marengo, J., 2009. Present-day South American climate. Palaeogeogr. Palaeoclimatol. Palaeoecol. 281, 180–195.
Grimm, E.C., 1987. CONISS: a FORTRAN 77 program for stratigraphically constrained cluster analysis by the method of incremental sum of squares. Comput. Geosci. 13, 13–35.
Grimm, E.C., 1992. Tilia, version 2.0.b.4 (Computer Software). Illinois State Museum. Research and Collection Center, Springfield.
Grimm, A.M., 2003. The El Niño impact on the summer monsoon in Brazil: regional processes versus remote influences. J. Clim. 16, 263–280.
Grimm, A.M., Pal, J.S., Giorgi, F., 2007. Connection between spring conditions and peak summer monsoon rainfall in South America: role of soil moisture, surface temperature, and topography in eastern Brazil. J. Clim. 20, 5929–5945.
Guy-Ohlson, D., 1992. Botryococcus as an aid in the interpretation of palaeoenvironment and depositional processes. Rev. Palaeobot. Palynol. 71, 1–15.
Horák, I., 2009. Relações pedológicas, isotópicas e palinológicas na reconstrução paleoambiental da turfeira da Área de Proteção Especial (APE) Pau-de-Fruta, Serra do Espinhaço Meridional - MG MSc Thesis Escola Superior de Sgricultura Luiz de Queiroz, Universidade de São Paulo, Brasil.
Horák-Terra, I., Martínez, Cortizas A., de Camargo, P.B., Silva, A.C., Vidal-Torrado, P., 2014. Characterization of properties and main processes related to the genesis and evolution of tropical mountain mires from Serra do Espinhaço Meridional, Minas Gerais, Brazil. Geoderma 232–234, 183–197.
Knauer, L.G., 2007. O Supergrupo Espinhaço em Minas Gerais: considerações sobre sua estratigrafia e seu arranjo estrutural. Geonomos 15, 81–90.
Kołaczek, P., Karpińska-Kołaczek, M., Worobiec, E., Heise, W., 2012. *Debarya glyptosperma* (De Bary) Wittrock 1872 (Zygnemataceae, Chlorophyta) as a possible airborne alga—a contribution to its palaeoecological interpretation. Acta Palaeobotanica 521, 139–146.
Ledru, M.-P., 1993. Late Quaternary environmental and climatic changes in Central Brazil. Quat. Res. 39, 90–98.
Ledru, M.-P., Salgado-Labouriau, M.L., Lorscheitter, M.L., 1998. Vegetation dynamics in southern and central Brazil during the last 10,000 yr B.P. Rev. Palaeobot. Palynol. 99, 131–142.
López-Merino, L., Silva Sánchez, N., Kaal, J., López-Sáez, J.A., Martínez Cortizas, A., 2012. Post-disturbance vegetation dynamics during the Late Pleistocene and the Holocene: an example from NW Iberia. Glob. Planet. Chang. 92–93, 58–70.
Machado, I.F., Figueirôa, S.F.M., 2001. 500 Years of mining in Brazil: a brief review. Resour. Policy 27, 9–24.
Marchant, R., Almeida, L., Behling, H., Berrio, J.C., Busch, M., Cleef, A., Duivenvoorden, M.K., Oliveira, P., Oliveira-Filho, A.T., Lozanogarcia, S., Hooghiemstra, H., Ledru, M.-P., Ludlow-Wiechers, B., Markgraf, V., Mancini, V., Paez, M., Prieto, A., Rangel, O., Salgado-Labouriau, M.L., 2002. Distribution and ecology of parent taxa of pollen lodged within the Latin America Pollen Database. Rev. Palaeobot. Palynol. 121, 1–75.
Markgraf, V., 1985. Paleoenvironmental history of the last 10,000 years in northwestern Argentina. Zent. Geol. Paläntol. 11–12, 1739–1749.
Markgraf, V., Anderson, L., 1994. Fire history of Patagonia: climate versus human cause. Revista do Instituto Geografico de São Paulo 15 pp. 33–47.
Martin, L., Flexor, J.M., Suguio, K., 1995. Vibrotestemunhador leve: construção, utilização e possibilidades. Rev. Inst. Geol. 16, 59–66.
Mendonça, R.C., Felfili, J.M., Walter, B.M.T., Silva Júnior, M.C., Rezende, A.V., Filgueiras, T.S., Nogueira, P.E., 1998. Flora Vascular do Cerrado. In: Sano, S.M., Almeida, S.P. (Eds.), Cerrado: ambiente e flora. Embrapa/CPAC, Brasília, pp. 289–556.
Montero-Serrano, J.C., Bout-Roumazeilles, V., Sionneau, T., Tribovillard, N., Bory, A., Flower, B.P., Ribouleau, A., Martinez, P., Billy, I., 2010. Changes in precipitation regimes over North America during the Holocene as recorded by mineralogy and geochemistry of Gulf of Mexico sediments. Glob. Planet. Chang. 74, 132–143.
Muller, J., Kylander, M., Wüst, R.A.J., Weiss, D., Martinez-Cortizas, A., LeGrande, A.N., Jennerjahn, T., Behling, H., Anderson, W.T., Jacobson, G., 2008. Possible evidence for wet Heinrich phases in tropical NE Australia: the Lynch's Crater deposit. Quat. Sci. Rev. 27, 468–475.
Nimer, E.C., 1977. Clima. Geografia do Brasil: Região Sudeste, Rio de Janeiro: IBGE, pp. 51–89.
Nobel, P.S., 1978. Microhabitat, water relations, and photosynthesis of a desert fern, *Notholaena parryi*. Oecologia 31, 293–309.
Parizzi, M.G., Salgado-Labouriau, M.L., Kohler, H.C., 1998. Genesis and environmental history of Lagoa Santa, southeastern Brazil. The Holocene 8, 311–321.
Reimann, C., Filzmoser, P., Garrett, R., Dutter, R., 2008. Statistical Data Analysis Explained: Applied Environmental Statistics with R. Wiley, Chichester.
Reimer, P.J., Bard, E., Bayliss, A., Beck, J.W., Blackwell, P.G., Bronk Ramsey, C., Buck, C.E., Cheng, H., Edwards, R.L., Friedrich, M., Grootes, P.M., Guilderson, T.P., Haflidason, H., Hajdas, I., Hatté, C., Heaton, T.J., Hoffmann, D.L., Hogg, A.G., Hughen, K.A., Kaiser, K.F., Kromer, B., Manning, S.W., Niu, M., Reimer, R.W., Richards, D.A., Scott, E.M., Southon, J.R., Staff, R.A., Turney, C.S.M., van der Plicht, J., 2013. IntCal13 and Marine13 radiocarbon age calibration curves 0–50,000 years cal BP. Radiocarbon 55, 1869–1887.
Roubik, D.W., Moreno, P.J.E., 1991. Pollen and Spores of Barro Colorado Island. Missouri Botanical Garden, New York.
Sánchez-González, A., Zúñiga, E.A., Tejero-Díez, J.D., 2010. Richness and distribution patterns of ferns and lycopods in Los Mármoles National Park, Hidalgo, Mexico. J.Torrey Bot.Soc. 137, 373–379.
Schoeneberger, P.J., Wysocki, D.A., Benham, E.C., Broderson, W.D., 1998. Field Book for Describing and Sampling Soils. Lincoln, Natural Resources Conservation Service, USDA, National Soil Survey Center.
Schuetz, L., 1989. Atmospheric mineral dust—properties and sources. In: Leinen, M., Sarthein, M. (Eds.), Pleocliamte and Paleometerorology: Modern and Past Patterns of Global Atmospheric Transport. Kluwer Academic Publishers, Netherlands, pp. 359–383.
Sehnem, A., 1970. Polipodiáceas. In: Reitz, R. (Ed.), Flora Ilustrada Catarinense. Itajaí, Herbário Barbosa Rodrigues, pp. 1–173.
Soil Survey Staff, 2010. Keys to Soil Taxonomy. Natural Resources Conservation Service, USDA, Washington.
Stríkis, N.M., Cruz, F.W., Cheng, H., Karmann, I., Edwards, R.L., Vuille, M., Wang, X., de Paula, M.S., Novello, V.F., Auler, A.S., 2011. Abrupt variations in South American monsoon rainfall during the Holocene based on a speleothem record from central–eastern Brazil. Geology 39, 1075–1078.
Taboada, T., Martínez Cortizas, A., García, C., García-Rodeja, E., 2006. Particle-size fractionation of titanium and zirconium during weathering and pedogenesesis of granitic rocks in NW Spain. Geoderma 131, 218–236.
Tryon, R.M., Tryon, A.F., 1982. Ferns and Allied Plants with Special Reference to Tropical America. Springer-Verlag, New York.
van Geel, B., 1976. A paleoecological study of Holocene peat bog sections, based on the analysis of pollen, spores and macro and microscopic remains of fungi, algae, cormophytes and animals PhD Thesis Universiteit van Amsterdam, Amsterdam.
van Geel, B., 1978. A palaeoecological study of holocene peat bog sections in Germany and The Netherlands, based on the analysis of pollen, spores and macro- and microscopic remains of fungi, algae, cormophytes and animals. Rev. Palaeobot. Palynol. 25, 1–120.
van Geel, B., Aproot, A., 2006. Fossil ascomycetes in Quaternary deposits. Nova Hedwigia 82, 313–329.
van Geel, B., Middeldorp, A.A., 1988. Vegetational history of Carbury Bog (Co. Kildare, Ireland) during the last 850 years and a test of the temperature indicator value of 2H/1H measurements of peat samples in relation to historical sources and meteorological data. New Phytol. 109, 377–392.
van Geel, B., Coope, G.R., van Der Hammen, T., 1989. Palaeoecology and stratigraphy of the late-glacial type section at Usselo (The Netherlands). Rev. Palaeobot. Palynol. 60, 25–129.
Vera, C., Higgins, W., Amador, J., Ambrizzi, T., Garreaud, R., Gochis, D., Gutzler, D., Lettenmaier, D., Marengo, J., Mechoso, C.R., Nogues-Paegle, J., Dias, P.L.S., Zhang, C., 2006. Toward a unified view of the American monsoon systems. J. Clim. 19, 4977–5000.
Wang, X., Auler, A.S., Lawrence Edwards, R., Cheng, H., Cristalli, P.S., Smart, P.L., Richards, D.A., Shen, C.-C., 2004. Northeastern Brazil wet periods linked to distant climate anomalies and rainforest boundary changes. Nature 432, 740–743.
Weiss, D., Cheburkin, A.K., Shotyk, W., 1998. Measurement of Pb in the ash fraction of peats using the EMMA miniprobe XRF analyzer. Analyst 123, 2097–2102.
Weiss, D., Shotyk, W., Rieley, J., Page, S., Gloor, M., Reese, S., Martinez-Cortizas, A., 2002. The geochemistry of major and selected trace elements in a forested peat bog, Kalimantan, SE Asia, and its implications for past atmospheric dust deposition. Geochim. Cosmochim. Acta 66, 2307–2323.
Ybert, J.P., Salgado-Labouriau, M.L., Barth, O.M., Lorscheitter, M.L., Barros, M.A., Chaves, S.A.M., Luz, C.F.P., Ribeiro, M.B., Scheel, R., Vicentini, K.F., 1992. Sugestões para padronização da metodologia empregada em estudos palinológicos do Quaternário. Bol. Inst. Geol. USP 13, 47–49.